5-1984

Structure and Petrology of Tertiary Volcanic Rocks in Parts of Toms Cabin Spring and Lucin NW Quadrangles (Box Elder Co.), Utah

Bruce Edward Scarbrough

STRUCTURE AND PETROLOGY OF TERTIARY VOLCANIC ROCKS IN PARTS OF TOMS CABIN SPRING AND LUCIN NW QUADRANGLES (BOX ELDER CO.), UTAH

by

Bruce E. Scarbrough

A thesis submitted in partial fulfillment
of the requirements for the degree

of

MASTER OF SCIENCE

in

Geology

Approved:

UTAH STATE UNIVERSITY
Logan, Utah
1984

ACKNOWLEDGEMENTS

I would like to extend my sincere thanks to my advisor and friend Dr. Donald Fiesinger, whose guidance, concern, and motivation made this project possible. Special thanks to my committee members Dr. Clyde Hardy and Dr. Peter Kolesar, whose assistance in both the field and laboratory was greatly appreciated, and to the Dept. of Geology for its financial support in the form of a teaching assistantship and research subsidy.

I would hate to think what Grouse Creek would have been like without the companionship and assistance of my good friend and collegue, Marc Olesen, whose friendship I will always cherish. Special thanks to all my fellow graduate students at Utah State University, who made my experience there one I shall never forget.

Thanks to Max and Melissa Tanner and Archie and Rhea of Grouse Creek, Utah, whose hospitality during the hot summer months made Marc and I feel at home. Thanks to the Dept. of Geology and Geophysics at the University of Utah for the use of the electron microprobe and XRF unit, and special thanks to Dr. Frank Brown for his assistance with the trace-element analyses. Thanks to Dr. David Dallmeyer of the University of Georgia for supplying radiometric age dates.

It is impossible to begin to acknowledge all of the love and support given to me by my parents during both my undergraduate and graduate years. Their unending faith in my abilities as both a student and a person allowed the completion of this goal.

Bruce E. Scarbrough

TABLE OF CONTENTS

TABLE OF CONTENTS (continued)

LIST OF TABLES

LIST OF FIGURES

LIST OF PLATES

ABSTRACT

Structure and Petrology of Tertiary Volcanic Rocks

in parts of Toms Cabin Spring and Lucin NW

Quadrangles (Box Elder Co.), Utah

by

Bruce Edward Scarbrough, Master of Science

Utah State University, 1984

Major Professor: Dr. Donald W. Fiesinger
Department: Geology

A series of late Tertiary rhyolitic and dacitic flows, domes, and minor pyroclastic rocks form an elongate volanic mass along the northwestern Utah-northeastern Nevada border. The structure of the flow banding and the linear arrangement of vents indicate that the mass represents a multi-sourced extrusive complex which erupted through many fissure-type conduits. A 39 km^2 area at the southern end of the mass was studied in detail in order to gain a better understanding of the eruptive nature and history of these Tertiary volcanic rocks. Age dating reveals that volcanism in the study area was episodic, and covered a period of at least 4 to 5 million years.

The silicic volcanic rocks in the study area are similar chemically and mineralogically to other eruptive units within the Rhyolite Mts., which range from dacite (SiO_2 69%) to high-silica rhyolite (SiO_2 75-77%). They also exhibit chemical characteristics similar to other silicic volcanic rocks of bimodal association in the western United States. Two-feldspar high-K rhyolite is the dominant volcanic rock in the study area, commonly found overlying

rhyolitic vitric tuffs and agglomerates. Rhyolite from the southern portion of the study area is dated at 7.6 to 8.6 m.y.b.p. Dacitic samples contain phenocrysts of plagioclase, quartz, biotite, hornblende, and orthopyroxene. Dacitic volcanism is dated at 12.4 m.y.b.p. By analogy with other "bimodal" volcanic fields in the western U.S., it is assumed that these silicic magmas are products of partial melting of crustal rocks. Evidence from a least squares differentiation model, along with the overall geochemical characteristics, indicates crystal fractionation as the dominant mechanism for the transition from dacite to rhyolite, with plagioclase as the dominant fractionating phase.

(77 pages)

INTRODUCTION

Purpose

An assemblage of Tertiary rhyolitic and dacitic lava flows, domes, and minor pyroclastic rocks, termed the Rhyolite Mountains (Doelling, 1980), forms a north-south trending mass of volcanic rocks in northwestern Utah and northern Nevada. These rocks represent the silicic endmember of bimodal basalt-rhyolite volcanism which was erupted widely in the Basin and Range Province during late Cenozoic time (Christiansen and Lipman, 1972).

A 39 km^2 area at the southern end of the Rhyolite Mountains was selected for study. The purpose of this study is to determine the structure and field relations of the rhyolites, dacites, and associated pyroclastic rocks found within the study area, along with their ages, mineralogy, and major- and trace-element compositions. This information is combined with similar data from previous work within the Rhyolite Mountains to develop a better understanding of the petrogenesis and eruptive history of these Tertiary volcanic rocks.

Location and Accessibility

The study area is located approximately 16 km southwest of the town of Etna, Utah in western Box Elder County (Fig. 1). The

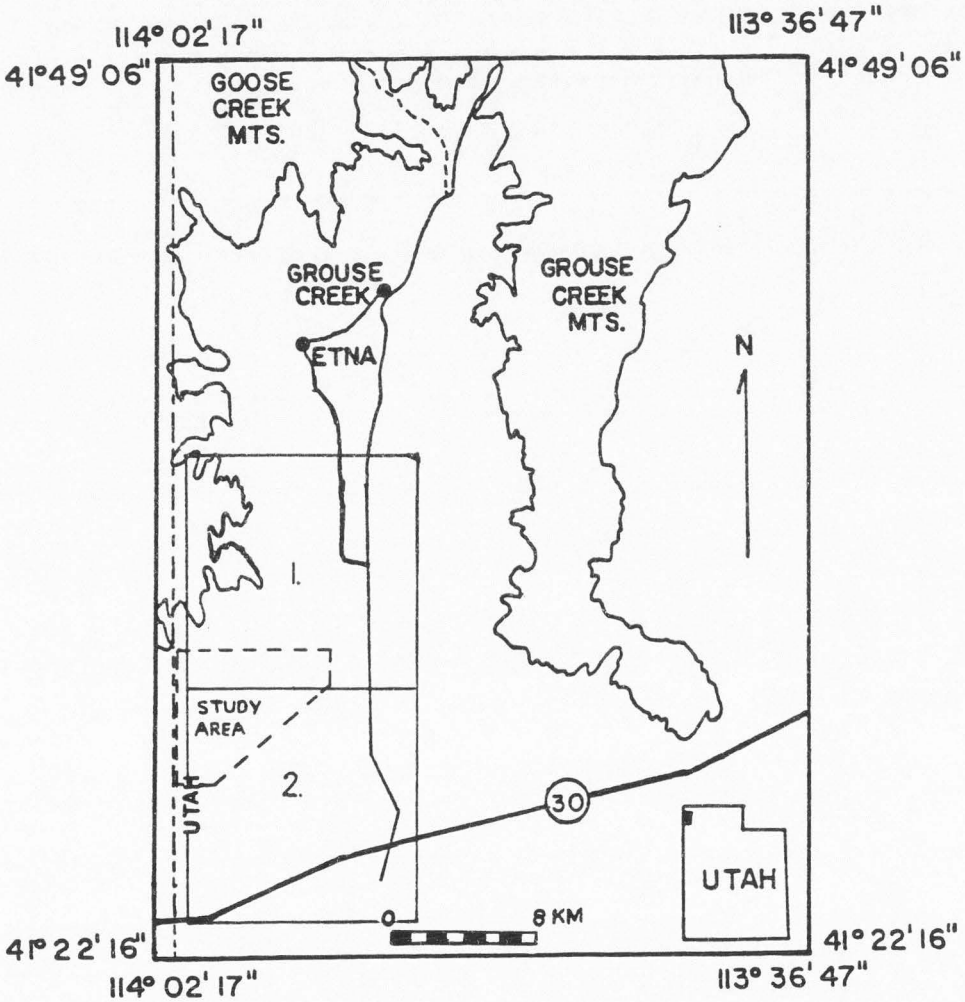

Fig. 1. Index map of study area.
1. Toms Cabin Spring quadrangle
2. Lucin NW quadrangle

39 km^2 area includes the northwestern portion of the Lucin NW quadrangle and the southern portion of the Toms Cabin Spring quadrangle. The western boundary extends to within 1.6 km of the Nevada state line, and the eastern boundary corresponds to the western edge of Grouse Creek Valley.

The area can be reached by following State Highway 30 for approximately 120 km west of Snowville, Utah, then north 8 km on an improved gravel road which parallels Grouse Creek Valley. Several unimproved dirt roads dissect the study area, allowing reasonable access to the entire area.

Grouse Creek Valley is a sparsely populated region in which the economy consists of agriculture and ranching. The land within the study area is primarily utilized by local ranchers for winter grazing of cattle (M. Tanner, Grouse Creek, Utah, pers. comm.).

Regional Geologic Setting

The Tertiary volcanic mass of which the study area is a part was termed the Rhyolite Mountains by Doelling (1980), and it lies within the northeastern portion of the Great Basin, a subprovince of the Basin and Range physiographic province (Fenneman and Johnson, 1946). This 29 km long north-south-trending volcanic mass defines the western boundary of Grouse Creek Valley, a trough-shaped depression approximately 48 km in length (Hood and Price, 1970). The valley is bounded on the east by the Grouse Creek Mountains, a complex uplifted structure composed of three allochthonous thrust sheets which have been thrust from west to east over a metamorphosed Pre-

cambrian autocthon during Cretaceous and possibly Late Jurassic time (Compton and others, 1977). Grouse Creek Valley is open to the south and drains to the Great Salt Lake Desert (Hood and Price, 1970). North and northwest of the Rhyolite Mountains lies the Goose Creek Range exposing Permian and Triassic sedimentary rocks, a large mass of Tertiary silicic volcanic rocks, and Tertiary sediments (Mapel and Hail, 1956).

The Rhyolite Mountains are situated in a region which underwent active late Cenozoic extension and subsequent high-angle normal faulting (McKee, 1971; Stewart, 1971; Nobel, 1972). In both the Goose Creek and Grouse Creek basins, the late Tertiary Salt Lake Formation is cut by normal faults with displacement ranging from a few feet to as much as 900 feet (Doelling, 1980).

The surface of Grouse Creek Valley at and below an elevation of 5180 feet has been modified by wave and current action of Pleistocene Lake Bonneville (Doelling, 1980). Quaternary lake deposits consist of clays and muds which dominate the intermontane valleys, and gravel deposits commonly found adjacent to isolated buttes and mountain range margins.

Previous Work

Geologic mapping of the grouse Creek Region was done by Stokes (1963) in preparing the state geologic map of Utah. The volcanic rocks of this region have generally been described as "Late Tertiary rhyolite-dacite-quartz latite flows," along with associated voluminous siliceous pryoclastic deposits. The most recent regional reconnaissance

and mapping was completed by Doelling (1980) in preparing a report of the geology and mineral resources of Box Elder County, Utah. In that publication, Doelling proposed the name Rhyolite Mountains for the Tertiary volcanic mass straddling the Utah-Nevada border.

More detailed studies on the structure and petrology of the volcanic rocks within the Rhyolite Mountains were carried out by Smith (1980) and Hare (1982). Both of these workers mapped the structure and distribution of rock types within areas north of the present study area. Smith (1980) studied the structure and petrology of three rhyolitic domes exposed approximately 10 km north of the present study area at Etna, Utah, while Hare (1982) looked at the structure and petrography of rhyolitic and dacitic flows and eruptive sites between Death Creek and Dairy Valley Creek.

Sampling Procedures and Analytical Methods

Field work consisted of geologic mapping of the study area and collecting fresh representative samples. A total of forty-two samples were collected from the study area. Following a petrographic study of all samples, four samples representative of the major rock types were chosen for further analysis. The locations of these four samples are presented in Table 1.

Modal analyses of these samples are based on 1,000 points per thin section. Whole-rock wet chemical analyses were performed on the four samples to determine major-element composition. Gravimetric, volumetric, and colorimetric methods as described by Maxwell (1968) were used. Trace-element analyses of the four representative

Table 1. Sample locations

Sample	Sample Location	Rock Type
LV82-4	41°30'37" N., 113°57'23" W.	Dacite vitrophyre
LV82-41	41°30'06" N., 113°57'57" W.	Dacite vitrophyre
LV82-19	41°29'50" N., 113°57'41" W.	Rhyolite
LV82-28	41°28'37" N., 113°58'47" W.	Rhyolite

samples along with other samples from the Rhyolite Mountains were obtained using a Phillips XRF unit at the Department of Geology and Geophysics, University of Utah.

Individual mineral and glass analyses were obtained using an ARL EMX SM electron microprobe at the Department of Geology and Geophysics, University of Utah. Feldspar phenocrysts were analyzed in all four samples in order to determine average endmember compositions. Complete analyses were performed on biotite, hornblende, orthopyroxene, and iron-titanium oxides present in dacitic samples. Microprobe analyses generally consisted of 50 spots per mineral, per sample. Correction procedures used on the microprobe data followed the methods of Bence and Albee (1968) and Albee and Ray (1970), and were carried out using computer programs developed by Nicholls et al. (1977). Corrections for glasses were made using an estimate of water content.

Radiometric dates for two dacitic and one rhyolitic sample were determined using biotite, hornblende, and sanidine separates. The rocks were radiometrically dated by R. D. Dallmeyer at the University of Georgia utilizing the Ar^{40}/Ar^{39} method.

ROCK UNITS

General Statement

Field mapping of the study area was completed during the summer months of 1982. Preliminary field reconnaissance determined significant mappable rock units in the study area. This was followed by detailed mapping of the distribution of these rock units along with the structure of internal flow banding and bedding surfaces.

The volcanic rocks of the study area can be divided into five mappable rock units. These are: (1) rhyolite; (2) rhyolite vitrophyre; (3) dacite; (4) dacite vitrophyre; and (5) pyroclastic rocks. Criteria used for distinguishing these rock units in the field were based on macroscopic mineralogical and textural features common to each unit.

Dacitic and rhyolitic rocks of the study area exhibit gross mineralogical differences which allow immediate recognition in the field. Glassy vs. crystalline groundmass is the major criterion utilized in differentiating vitrophyre from its crystalline equivalent.

Sedimentary rock units exposed in the study area are the Tertiary Salt Lake Formation, and recent unconsolidated alluvial and colluvial deposits.

Igneous Rocks

Rhyolite

Rhyolite comprises the bulk of the volcanic rocks exposed in the study area. The entire southern portion of the map area is composed of rhyolitic flows and eruptive centers, along with their associated pyroclastic deposits.

All rhyolitic samples are porphyritic with phenocrysts of quartz, feldspar, and less commonly ferromagnesian minerals. The presence of abundant large quartz phenocrysts (1-4 mm diameter), and the absence of abundant ferromagnesian minerals distinguish rhyolite from dacite in the field.

Fresh samples of rhyolite are variable in color, ranging from light gray to moderate red. Weathered outcrops range in color from medium brown to pale orangish brown. Weathering of rhyolite commonly results in rounded, oblong-shaped outcrop patterns with zones of rough and pitted surfaces caused by weathering of lithophysae.

Textures within rhyolite are also variable. The main body of the rhyolitic flows is foliated with fluidal structure. The foliation generally consists of vari-colored laminae about 1-3 mm in thickness. Within the crystalline rhyolite, the flow banding is commonly marked by either partially glassy layers between completely devitrified layers, or simple partings between similar layers of rock. Foliations of this nature were observed in rhyolite lava flows in southern Nevada described by Christiansen and Lipman (1966).

Massive, non-foliated rhyolite which appears to have a slightly

higher percentage of phenocrysts is less common, and generally grades directly into a foliated section. Autobreccias are found in the study area. They are commonly extensively silicified, and make up small isolated mounds possibly representing a flow surface whose continuity has been destroyed by erosion. Autobreccias are volcanic flow breccias formed by the fragmentation of a chilled flow surface by continued movement of still-fluid lava below (Parsons, 1969).

Rhyolite vitrophyre

Rhyolite vitrophyre represents a quickly chilled layer commonly found along the base and margins of flow units. These relatively thin layers never exceed 40 feet in vertical thickness and are found locally grading into the main crystalline body of a rhyolite flow.

The phenocryst assemblage of rhyolite vitrophyre is similar to that of rhyolite, with quartz and sanidine the dominant phases. In hand sample, vitrophyre is composed of large (1-4 mm diameter) quartz and feldspar phenocrysts set in a black, glassy groundmass. The distinctive black glass and the presence of abundant quartz phenocrysts distinguishes rhyolite vitrophyre from dacite vitrophyre.

Fresh outcrops of rhyolite vitrophyre are black in color. Weathering of virtophyre generally does not result in any change in color, but commonly produces a crumbly, friable texture. Devitrification of the glass commonly can be seen in hand sample in the form of light grey spherulites up to 5 mm in diameter.

Textural variations within the rhyolite vitrophyre can best

be seen in a basal rhyolite vitrophyre found directly overlying a sequence of genetically related pyroclastic rocks in Sec. 26, R.19W., T.9N. The base of the vitrophyre flow unit consists of a flow breccia containing angular clasts of glassy rhyolite vitrophyre set in a matrix of dense glass. The basal unit lies directly on a lithic tuff breccia containing fragments of rhyolite identical to the overlying flow. The contact between the flow breccia and the tuff breccia is locally sharp. The lower flow breccia locally grades upwards into the overlying main body of the flow unit, which is a dense foliated rhyolite vitrophyre with tabular, slightly inclined flow banding. The basal vitrophyre unit in turn grades upwards into a crystalline, foliated rhyolite in which the flow banding is generally inclined, contorted, and discontinuous.

Dacite

Dacite is much less abundant than rhyolite, and is restricted to isolated buttes and several large ridges in the north-central portion of the study area. Areally, dacite covers approximately 4 km^2 of the study area.

Field identification of dacite is based on the absence of large quartz phenocrysts and the presence of abundant ferromagnesian minerals. Phenocrysts of feldspar, along with smaller phenocrysts of hornblende and biotite are commonly visible in hand sample and are set in a microcrystalline to granular groundmass.

Fresh dacitic samples range in color from pale pink to light gray, and are generally streaky in appearance. The color variations in weathered dacite generally reflect the degree of oxidation of the

ferrogmagnesian minerals, and colors range from moderate reddish brown to dark reddish brown.

Dacite commonly exhibits fluidal structure similar to rhyolite. Foliation surfaces within the rock result from flowage, and are marked by differences in color and texture. Massive, non-foliated sections of dacite are rare, and generally grade directly into a foliated section.

Dacite vitrophyre

Dacite vitrophyre represents the glassy equivalent of the crystalline dacite, and reflects a difference in cooling history. The glassy groundmass present in vitrophyre results from rapid cooling, prohibiting crystallization of the liquid phase (Stewart, 1979). Dacite vitrophyre is most commonly found capping a larger unit of crystalline dacite, but in one case, a mass of dacite vitrophyre is found directly overlying a rhyolitic tuff sequence in a relatively high topographic position. Basal dacite vitrophyre is rarely exposed in the study area.

The phenocryst assemblage of dacite vitrophyre is similar to that of crystalline dacite, though commonly vitrophyre contains a greater percentage of mafic phenocrysts, especially hornblende. In hand sample, the dacite vitrophyre can easily be distinguished from rhyolite vitrophyre on the basis of absence of quartz phenocrysts and the presence of abundant mafic phenocrysts.

Fresh outcrops of dacite vitrophyre are light gray to dark gray in color with little variability. Weathering of the vitrophyre results in the formation of a dark-brown to dull black resinous

rind. Devitrification of the glassy groundmass in the form of reddish-brown spherulites up to 1 mm in diameter occurs locally, but is not a widespread feature.

Textures within dacite vitrophyre exhibit little variability. On a macroscopic scale the vitrophyre commonly appears to lack flow banding features, but microscopic examination reveals curving trains of microlites and parallel alignment of phenocrysts resulting from flowage.

Pyroclastic rocks

The volcanic rock units mapped as pyroclastic rocks are those considered to be genetically related to the adjacent crystalline and glassy lavas. These rocks include well-bedded tuffs and massive agglomerates. Evidence supporting a genetic relation to overlying lava flows include: (1) their areal distribution is similar to that of the lavas; (2) they contain blocks of rhyolite identical to the overlying lavas, and commonly grade up into flow breccias at the base of a lava flow; and (3) their phenocryst mineralogy is similar to that of the lavas.

A thick continuous sequence of pyroclastic rocks underlies a rhyolite vitrophyre unit in the southwestern portion of the study area. This sequence is composed primarily of interbedded vitric and lithic tuffs which generally are well bedded, and commonly exhibit normal graded bedding. The tuffaceous units range from well-sorted vitric tuffs to poorly sorted lithic tuffs containing angular clasts of rhyolite. Accretionary lapilli composed of fine

ash are found within vitric tuffs, and possibly were formed by the accretion of glass dust onto rain drops. The sequence also contains units of massive to poorly bedded volcanic agglomerates composed of subequant pumiceous and vitrophyric clasts in a fine glassy matrix.

Sedimentary Rocks

Salt Lake Formation

The Salt Lake Formation is believed to range in age from late Eocene to late Pliocene (Smith and Nash, 1976). These heterogenous rocks consist of deposits of fluvial, lacustrine, and volcanic origin. Within the Grouse Creek basin, the Salt Lake Formation consists primarily of mudstone, shale, conglomerate, and interbedded volcanic ash (Doelling, 1980).

The Salt Lake Formation is exposed as low-lying rounded mounds in the far northwestern portion of the study area. Of the numerous rock types characteristic of Salt Lake Formation, only conglomerate and non-welded tuffaceous rock are found in the study area. The tuffaceous rock is a non-welded, well-bedded, friable volcanic ash, ranging in color from light gray to pale greenish yellow. The conglomerate, which appears to overlie the tuff, is medium gray and contains well-rounded pebbles of quartzite and chert in a fine-grained matrix. The conglomerate contains no volcanic fragments and, therefore, is believed to predate the volcanism. The conglomerate is also extensively silicified.

STRUCTURE

Rhyolite

Rhyolite flows and dome-like eruptive centers, along with genetically related pyroclastic rocks are the most abundant volcanic rocks exposed in the study area. In general, rhyolite exhibits a conspicuous flow banding imparted during the liquid or plastic stage. The distribution of foliation patterns within rhyolite is the main criterion utilized in interpreting structural relations and identification of eruptive centers.

The southern and central portions of the study area are comprised of several large rhyolitic flows and eruptive centers. Distinguishing separate flow units is very difficult due to the extreme variability of foliation patterns and the lithologic homogeneity within the rhyolite.

Although no voluminous ash deposits, characteristic of large-scale caldera collapse, are exposed, a section of non-welded, bedded vitric and lithic tuffs and massive agglomerates is exposed throughout the southern portion of the study area. This coherent unit of ash-flow tuffs is found continuously underlying rhyolite vitrophyre. These pyroclastic deposits are thought to represent the more highly gas-charged portions of the magma erupted from the upper portion of a magma chamber.

The rhyolite and rhyolite vitrophyre directly overlying tuffaceous deposits in the NE 1/4, Sec. 26, T.9N., R.19W. were dated by Armstrong et al. (1976) at 8.6 and 8.2 m.y.b.p., respectively. The extrusions

were viscous, flow-layered rhyolite domes and stubby flows. Numerous indications of closures in the flow banding throughout the area indicate the presence of multiple sites of eruption. One distinct dome-shaped eruptive center is shown in cross-section A-A' (Plate 1). In this dome, the concentric structure is emphasized by short, arcuate ridges which exhibit consistent steeply inclined flow banding. The flow banding flattens toward the periphery of the dome, with low dips both inwards and outwards. The other conspicuous rhyolitic eruptive site is found in SE 1/4, of Sec. 24, T.9N., R.19W. Like the previously discussed eruptive center, this site is composed of large arcuate ridges with near vertical flow banding, yet it lacks the concentric structure of a volcanic dome.

A series of north-south trending rhyolite ridges extends along the entire western edge of the study area. The foliation patterns tend to strike parallel to the ridge margins, and although the flow banding is not always vertical, the consistency of trends indicates a linear arrangement of multiple vents.

The rhyolite exposed in the north-central portion of the study area lacks any conspicuous structure and is commonly extensively brecciated and silicified. The structural field relations indicate that this same rhyolite has been intruded and is overlain by younger dacitic volcanic rocks. A dacite vitrophyre from this eruptive unit was radiometrically dated at 12.4 $\pm$ 0.4 m.y.b.p. (Dallmeyer, University of Georgia, pers. comm.). This indicates that at least two stages of rhyolitic volcanism are represented in the study area.

Dacite

Dacite eruptive centers and flows are restricted to the north-central and northeastern portions of the study area. Dacitic tuffs associated with dacitic flows are abundant directly north of the study area (M.H. Olesen, Utah State University, pers. comm.), but none have been identified within the study area.

A distinct system of closely spaced fissure-eruption centers has been located in the northern portion of the study area. Cross section B-B' reveals dacitic fissure-eruptive centers found along ridge crests in the southern portion of Sec. 12, T.9N., R.19W. In this case the dacite appears to have intruded through an older rhyolite terrain as mentioned previously. The large arcuate ridge located in the NW 1/4 of Sec. 13, T.9N., R.19W. also exhibits consistent inclined flow banding dipping steeply to the south and east. The large dacite ridge in Sec. 7, T.9N., R.18W. is dominantly composed of crystalline dacite and is also considered to be an eruptive site. The foliation patterns along the ridge crest do not parallel the ridge, but do exhibit consistent vertical or near-vertical inclination. This ridge extends north of the study area, and is also interpreted to be a fissure-eruptive center by M.H. Olesen (Utah State Univ., pers. comm.). Dacite vitrophyre found along ridge crests commonly exhibits vertical foliation comformable with crystalline dacite, and is considered to be preserved portions of the erupted dacite which were supercooled.

Faults

The linear trend of the Rhyolite Mountains and the existing topography indicates that the volcanism was strongly fault controlled. Strong evidence for normal faulting along the western margin of Grouse Creek Valley exists in the form of a series of steep linear scarps along the eastern margin of the volcanics. The eastern margin of the large north-south trending ridge in Sec. 7, T.9N., R.18W. represents the southern extension of a normal fault system which extends north along the valley margin into the areas studied by Hare (1982), and Olesen (Utah State University, pers. comm.). The extension of the fault into the study area is inferred, but the presence of steep planar walls along the southeastern end of the ridge supports the presence of a normal fault.

A small northwesterly-trending high-angle fault is located in the far southwestern portion of the study area. The fault trends approximately N20W and cuts a sequence of rhyolitic tuffs directly underlying the rhyolitic eruptive center. The fault displaces the tuff sequence approximately 80 feet, with the downthrown block to the northeast. The fault postdates deposition of the tuffs and the overlying rhyolite, but cannot be traced into the rhyolite unit.

Mode of Emplacment and Origin

The linear trend of both the rhyolite and dacite vents, along with the structure of flow banding, indicates that both magmas were emplaced passively through multiple tabular conduits. Fink and Pollard (1983) have suggested that the linear distribution of silicic vents at various volcanoes in the western United States can be attributed to the presence of elongaged subsurface conduits. The segmented and en echelon nature of the domes and fissure-eruptive centers supports this hypothesis, since dikes commonly are composed of en echelon segments (Delaney and Pollard, 1981).

The distribution of the silicic vents in the study area can also be related to the dominant style of tectonism during the time of volcanism. Regional north-northwest-trending crustal extension is characteristic of the Great Basin during the late Tertiary (McKee, 1971; Stewart, 1971; Nobel, 1972). An extensional stress pattern characterized by high-angle block faulting would also facilitate the formation of elongate subsurface conduits through which dike-like bodies of silicic magma could reach the surface. The overall alignment of domes and fissure-eruptive centers wihin the study area and the Rhyolite Mountains as a whole, seems to indicate a tabular feeder-vent geometry.

GEOCHRONOLOGY

To determine the age of volcanic activity and to establish the geologic relations between eruptive units, two samples from the study area and one directly adjacent to it were radiometrically dated. A summary of these dates and sample locations along with other dates from the Rhyolite Mts. are presented in Table 2.

The youngest flows of the study area are rhyolites from the southern portion of the study area. Samples YU-1A-AY and YU-1-AY are rhyolite vitrophyre and overlying crystalline rhyolite dated by Armstrong et al. (1976) at 8.6 and 8.2 m.y.b.p., respectively. Sample LV82-28, a crystalline rhyolite, was collected from the same unit and considered to be the same age. Another rhyolite from the southern portion was dated by Dallmeyer (Univ. of Georgia, pers. comm.) at 7.6 m.y.b.p. Although this date corresponds closely to Armstrong's, the small amount of sanidine recovered from the sample makes it suspect (Dallmeyer, University of Georgia, pers. comm.). These dates seem to define an episode of rhyolitic volcanism which took place within a short period of time about 8.0 m.y ago.

Dacite sample LV82-41 yielded a date of 12.4 m.y.b.p., and indicates a considerable amount of time between dacitic and the rhyolitic volcanism to the south. Another dacite (TCV82-55) located to the north in Olesen's study area was dated at 13.2 m.y.b.p., corresponding closely to the date determined on LV82-41. The dacite of the study area, and those exposed to the north are found to locally overlie rhyolite. This stratigraphic relation indicates that

Table 2. Radiometric ages from the Rhyolite Mts., Utah

Sample	Rock Type	Sample Location	Age (m.y.)
LV82-41[1]	Dacite Vitro.	41°30'06" N., 113°57'57" W.	12.4±0.40
TCV82-55[1]	Dacite Vitro.	41°32'26" N., 113°59'35" W.	13.2±0.50
LV82-19[1]	Rhyolite	41°29'50" N., 113°57'41" W.	7.6±0.90
YU-1A-AY[2]	Rhyolite Vitro.	41°28'32" N., 113°59'15" W.	8.6±0.17
YU-1-AY[2]	Rhyolite	41°28'32" N., 113°59'13" W.	8.2±0.16

1 Dated by R.D. Dallmeyer (Univ. of Georgia, pers. comm.).
2 Armstrong et al. (1976).

a period of rhyolitic volcanism also occurred prior to the dacitic volcanism, but no age dates on these older rhyolites are available to substantiate this.

PETROGRAPHY

General Statement on Textures

All of the igneous rocks studied exhibit a markedly porphyritic texture. A common feature to all of the porphyritic rocks studied is the presence of cumulophyric aggregates. Based on the morphology of the aggregates, they are interpreted as synneusis structures, and provide a ready criterion supporting a magmatic origin (Vance, 1969).

The groundmass of all the samples collected from the study area can be divided into three descriptive textural varieties: (1) vitrophyric; (2) felsophyric; and (3) spherulitic-axiolitic. Vitrophyric rocks exhibit a dense, glassy groundmass which is clear to reddish brown, and commonly contains abundant concentric perlitic cracks along which incipient devitrification has occurred. Fluidal banding accentuated by curving trains of rod-like crystallites or lath-shaped microlites is a conspicuous feature common to all vitrophyres studied.

Felsophyres are characterized by a microcrystalline granular groundmass composed of interlocking quartz and feldspar commonly stippled with hematite dust. Spherulites range from 0.05 to 5.0 mm in diameter, and are composed of acicular crystals of feldspar and cristobalite. Axiolites occur when spherulite fibers do not radiate from a common point, but from a line of greater or lesser length (Teall, 1888). The size and morphology of individual crystals within spherulites or axiolites varies from broad tabular

fibers or branches to finer closely spaced fibers. Some of the rocks contain a relatively few, isolated, large spherulites, while others exhibit a dense complexly intergrown microspherulitic texture only visible microscopically by their sweeping extinction patterns. Spherulitic-axiolitic and felsophyric textures commonly occur together in the same rock and possibly represent two distinct phases of devitrification as proposed by Lofgren (1971).

Textures similar to those observed in the rhyolites and dacites of the study area have been experimentally produced by crystallizing liquids of rhyolitic composition by either isothermal drops (Svanson, 1977; Lofgren, 1976), or cooling (Lofgren, 1976). Devitrification of a natural rhyolite glass under experimental conditions also produced similar spherulitic and felsophyric textures (Lofgren, 1971). Thus, distinguishing devitrification from primary crystallization textures can be difficult without the presence of a sharp devitrification front. Several of the glassy rocks studied showed widely spaced spherulites which obviously crystallized at subsolidus temperatures, as evidenced by the presence of curving crystallites passing undisturbed through spherulite bodies.

Rhyolite

All of the rhyolites samples collected from the study area are mineralogically very similar, with noted differences in groundmass texture. The majority of rhyolites sampled exhibit a felsophyric and or spherulitic-axiolitic groundmass, with vitrophyres much less common.

Samples LV82-19 and LV82-28 were classified in the field as rhyolites and chosen as representative rhyolitic samples. They contain phenocrysts of quartz, sanidine, plagioclase, and less commonly biotite and iron-titanium oxides in a felsophyric to microspherulitic groundmass. The groundmass of LV82-19 contains abundant wedge-shaped tridymite crystals infilling cavities. The presence of fayalitic olivine as an accessory mineral is limited to some of the rhyolites collected from the southern portion of the study area. This is the only example of a specific mineral being exclusive to certain rhyolites. Other common accessory minerals found in rhyolitic samples throughout the study area are zircon, allanite, and apatite.

Average modal analyses of samples LV82-19 and LV82-28 show them to contain 14.3% quartz, 11.2% sanidine, and 2.7% plagioclase (Table 3). The microcrystalline nature of the groundmass of these samples prohibits an accurate classification based solely on modal constituents, therefore, chemical criteria were utilized for classification purposes. Details of the classification scheme will be discussed later in the text.

The most widespread type of post-intrusion alteration observed

Table 3. Modal analyses of representative samples (volume percent)

	Dacite Vitrophyre		Rhyolite	
	LV82-4	LV82-41	LV82-19	LV82-28
Quartz	1.1	--	13.4	15.2
Sanidine	--	--	11.8	10.6
Plagioclase	19.5	21.5	3.6	1.9
Biotite	2.5	0.8	--	--
Amphibole	3.3	2.8	--	--
Orthopyroxene	1.7	3.7	--	--
Fe-Ti oxides	1.0	1.3	0.7	0.2
Glass Groundmass	70.2	69.7	--	--
Felsophyric Groundmass	--	--	70.5	71.5
Accessory*	0.7	0.2	tr.	0.6

* Accessory minerals consist of allanite, zircon, apatite, fayalitic olivine

within the rhyolites is the presence of opal and chalcedony infilling cavities and fractures within the crystalline groundmass. These silica products are not found in vitrophyric rhyolites, and therefore, it is inferred that they result from the deposition of silica by residual solutions or meteoric waters.

Dacite

Samples LV82-4 and LV82-41 were classified in the field as dacite vitrophyres and found to contain phenocrysts of plagioclase, biotite, hornblende, orthopyroxene, and iron-titanium oxides in a dense, clear, glassy groundmass. Quartz is found as a minor phenocryst phase in sample LV82-4, but it is absent in LV82-41.

The glassy groundmass of sample LV82-4 is filled with hair-like crystallites which wrap around phenocrysts and commonly form circular eddy zones on the downflow side of phenocrysts. This sample also contains abundant concentric perlitic cracks along which devitrification has occurred. The glass in sample LV82-41 lacks perlitic structures and is peppered with abundant feldspar microlites often showing a subparallel arrangement, but more commonly a radiating texture.

Average modal analyses of LV82-4 and LV82-41 show them to contain 20.5% plagioclase, 1.7% biotite, 2.7% orthopyroxene, and 1.1% iron-titanium oxides (Table 3). As in the rhyolites, classification of these glassy rocks on the basis of modal phenocryst assemblage is inappropriate.

Felsophyric and spherulitic-axiolitic dacite exhibits similar mineralogy to that of virtophyric dacite, yet its greater suscep-

tibility to secondary alteration has resulted in the nearly complete oxidation of the ferromagnesian minerals. Also, its crystalline groundmass has commonly been partially replaced or altered and exhibits a granular to microcrystalline texture. The extensive silification features present in rhyolite are not found in any of the dacitic samples.

Pyroclastic Rocks

The associated pyroclastic deposits generally found underlying rhyolite vitrophyre vary from very well-sorted vitric tuffs, to poorly-sorted lithic tuffs and agglomerates. All of these fragmental rocks contain abundant glass in the form of bubble-wall shards, pumice shards, or as a binding dusty matrix. Devitrification of glass fragments is variable, but much more complete in the fine-grained glassy matrix.

The well-sorted vitric tuffs are generally composed of a framework of little-abraded bubble-wall glass shards, averaging less than 0.10 mm, set in an aphanitic glassy groundmass. Anhedral to subhedral crystals and crystal fragments of plagioclase, sanidine, quartz, and ferromagnesian minerals are common but never exceed one or two volume percent of the rock.

The lithic tuffs and agglomerates, which comprise the largest volume of the pyroclastic deposits, are composed of subequant vitrophyric and felsophyric rhyolitic rock fragments and pumice clasts, set in a glassy groundmass of pumice shards and dust. The rock fragments and pumice clasts range from 1.0 to 0.3 meters in diameter. Pumice clasts are commonly flattened, stretched, and

imbricated, indicating some degree of flow transport. Crystals and crystal fragments of quartz, plagioclase, sanidine, and ferromagnesian minerals are also common minor constituents.

Extensive silification is a common post-depositional alteration within the pyroclastic deposits. Opal and chalcedony occur as both microcrystalline cement infilling pore spaces and as discrete veins and nodules. Silicified horizons are dense and brittle, while the unaltered horizons remains friable and extremely porous. Silica released from the alteration of volcanic glass, or infiltration of silica-rich solutions represent the major sources of silica.

Minerals

Plagioclase

Phenocrysts of plagioclase are found in all of the dacitic and rhyolitic samples studied, and frequently occur as rounded crystals within pyroclastic units. Plagioclase microlites appear as an abundant groundmass phase in sample LV82-41, a dacite vitrophyre. Plagioclase abundances are 15.0 and 23.0 volume percent in the two dacitic samples, and 0.5 and 3.0 volume percent in the two rhyolitic samples.

Plagioclase phenocrysts within rhyolite commonly occur as subhedral to anhedral crystals ranging from 0.3 to 3.0 mm in maximum diameter, with an average of 1.0 mm. Plagioclase in dacitic samples exhibits a distinctly bimodal size distribution representing two generations of plagioclase crystallization. The smaller, more abundant microphenocrysts range from 0.2 to 1.0 mm in length, and frequently occur as euhedral laths. The larger plagioclase phenocrysts vary from anhedral to euhedral crystals, and range from 1.0 to 6.0 mm in diameter, with an average of 2.5 mm.

Twinning in plagioclase is common in both rhyolitic and dacitic rocks. Albite twinning and the combined albite-Carlsbad twin are the most common, especially among the larger phenocrysts, while the simple Carlsbad twin is prevalent among the smaller phenocrysts in dacite. Oscillatory zoning is characteristic of nearly all plagioclase phenocrysts in dacitic samples, and is especially evident in the larger sized generation of plagioclase. Plagioclase in

rhyolitic samples is frequently corroded and contains glassy bleb-like inclusions, yet lacks extensive zonation. A common feature of nearly all dacitic samples is the presence of large phenocrysts which have undergone extensive internal resorption and subsequent mantling by fresh euhedral overgrowths. The dacite microphenocrysts are rarely corroded, and apparently were not subjected to the same disequilibrium conditions.

Plagioclase has a strong tendency to form cumulophyric aggregates with other plagioclase phenocrysts, and less commonly sanidine and ferromagnesian minerals, yet appears to have a strong antipathy for preferential synneusis with quartz. This textural feature was explained by Vance (1969) as a result of lack of permanent contact between the two minerals until final stages of crystallization.

Sanidine

Sanidine is a ubiquitous phenocryst phase in all rhyolitic samples, and absent in all dacitic samples. Phenocryst abundances in the two rhyolites are 10.6 and 11.8 volume percent. Sanidine is also present as a groundmass constituent in felsophyric and spherulitic-axiolitic samples. Spherulites and axiolites are composed of acicular sanidine and cristobalite crystals.

Phenocrysts within the rhyolites range from 0.2 to 5.0 mm along the maximum crystal dimension, with an average of 1.5 mm. Shapes vary from euhedral laths or square sections to the more common rounded and embayed subhedral crystals. Sanidine commonly forms large cumulophyric aggregates with other crystals of sanidine,

and less commonly plagioclase and quartz. Simple twinning following the Carlsbad law is common among the larger phenocrysts. Zoning within sanidine is not petrographically discernible. In a few rhyolite samples granophyric intergrowths of quartz and sanidine occur in megacrysts. Quartz intergrowths vary in habit from cuneiform to vermicular, and often exhibit uniform optical orientation. These intergrowths are found in both vitrophyric and felsophyric rhyolites.

Quartz

Excluding dacite sample LV82-41, quartz is present as a phenocryst phase in all of the rocks examined. Quartz exists as a common groundmass constituent in felsophyric and spherulitic-axiolitic rocks as interlocking microcrystalline grains intergrown with feldspar. Tridymite, along with secondary opal and chalcedony, are common vug and cavity fillers within felsophyric rhyolites. The abundance of quartz phenocrysts in the two rhyolites is 13.4 and 15.2 volume percent, while quartz is present in one of two dacites at 1.1 volume percent (Table 3).

Quartz phenocrysts range in size from 0.10 to 4.0 mm in diameter, and average 2.0 mm within rhyolite; they range from 0.3 to 2.0 mm with an average diameter of 1.0 mm within dacite. The quartz phenocrysts are generally anhedral and have been rounded and embayed by extensive magmatic corrosion. Commonly quartz is embayed, resulting in glass-filled cavities. The presence of stubby, subhedral, hexagonal, bipyramidal crystals indicates original crystallization as β-quartz

at a temperature above 573 degrees Celsius (Phillips and Griffen, 1981).

Amphibole

Hornblende is a ubiquitous phenocryst phase in all dacitic samples, but only occurs as a rare accessory mineral in rhyolite. Subhedral crystals of hornblende are also found in some of the pyroclastic units. Abundances of hornblende are 2.8 and 3.3 volume percent for the two dacitic samples (Table 3).

Hornblende appears as subhedral to euhedral phenocrysts commonly in the form of rectangular prismatic sections and diamond-shaped basal sections. The prismatic sections range from 0.3 to 1.5 mm in length, with an average length of 1.0 mm. The prismatic sections are commonly aligned parallel to subparallel with the flow direction and define a distinct lineation.

Pleochroism in the hornblende varies from shades of green to shades of brown. Hornblende with a distinctive dark reddish-brown pleochroism is commonly present in dacites with a microcrystalline groundmass. This strong reddish-brown pleochroism is characteristic of oxyhornblende, and likely represents the oxidized product of common hornblende. Common hornblende can be transformed to oxyhornblende upon heating to 800 degrees Celsius (Barnes, 1930, as cited in Deer et al., vol. 2, 1963). Oxyhornblende commonly exhibits alteration rims of fine granular aggregates of black iron oxides and pyroxene. A common feature of hornblende is the frequent cumulophyric relationship with plagioclase, pyroxene, and iron-titanium

oxides.

Biotite

Similar to hornblende, biotite is also a ubiquitous phenocryst phase in dacitic samples, and occurs as a common accessory in rhyolites though never exceeding 0.5 volume percent. Abundances in dacitic samples are 0.8 and 2.5 volume percent.

Biotite phenocrysts commonly occur as subhedral to euhedral hexagonal or prismatic forms ranging from 0.2 to 2.5 mm in length. The prismatic sections frequently align themselves parallel with the direction of flow, defining a distinct lineation most easily recognizable in sections cut perpendicular to flow banding. Biotite exhibits a strong pleochroism in shades of green and brown, but may be completely altered to opacity.

Pyroxene

Orthopyroxene is a common mafic phenocryst phase in dacitic samples, especially dacite vitrophyres. Abundances in the two dacites are 1.7 and 3.7 volume percent. Pyroxenes are very uncommon in rhyolitic samples with the exception of one sample of rhyolite vitrophyre which contains approximately 0.5 percent clinopyroxene.

Orthopyroxene forms euhedral prismatic or square cross-sectional crystals, with a maximum length of 1.0 mm and a distinctive light-green to pale-pink pleochroism. Pyroxene found in non-glassy dacite commonly has oxidized rims of granular opaque minerals. Orthopyroxene

frequently occurs as isolated grains, but also has a strong preference to form clusters with other pyroxene and iron-titanium oxides. Commonly iron-titanium oxides occur as inclusions with pyroxene grains.

Iron-titanium oxides

Iron-titanium oxides are present in all of the dacitic samples, and are commonly found in rhyolitic samples. Abundances in dacite are 1.0 and 1.3 volume percent. Iron-titanium oxides never exceed 1.0 percent in rhyolite.

Rhyolitic samples seldom contain large euhedral crystals of iron-titanium oxides; however, they commonly exhibit microscopic grains disseminated throughout the groundmass. In dacite, the iron-titanium oxides are subhedral to euhedral equidimensional grains ranging in diameter from 0.05 to 0.6 mm, with an average of 0.2 mm. The iron-titanium oxides commonly form inclusions in biotite, hornblende, and pyroxene phenocrysts, and exhibit a strong tendency to form aggregates with ferromagnesian minerals.

Olivine

Iron-rich olivine is present as an accessory phase within rhyolite from the southern-most portion of the study area. Abundances are less than 0.2 volume percent.

The fayalitic olivine phenocrysts occur as subhedral, highly fractured equant grains, with a maximum diameter of 0.5 mm. In

felsophyric and spherulitic-axiolitic rocks, such as sample LV82-28, fayalitic olivine is almost completely destroyed by oxidation and hydration to iddingsite, and even within vitrophyre, fayalitic olivine is oxidized peripherally and along fractures.

MINERALOGY

General Statement

Microprobe analyses were carried out on polished probe mounts of the four selected samples. The two rhyolitic samples, LV82-19 and LV82-28, contain no fresh ferromagnesian phases and the iron-titanium oxides were oxidized and exsolved; therefore, mineral analyses of the rhyolites were restricted to the determination of respective major oxides required for endmember compositions of sanidine and plagioclase phenocrysts. Phenocryst phases of biotite, amphibole, and co-existing iron-titanium oxides in dacitic samples were analyzed for their respective major oxides. Both generations of plagioclase, along with orthopyroxene phenocrysts, were analyzed for major oxides required for endmember compositions.

Feldspars

Plagioclase

Average microprobe analyses for plagioclase in dacitic and rhyolitic samples are presented in Table 4 and are plotted in Fig. 2. Both generations of plagioclase within dacite were analyzed, and the data are presented separately.

The large, skeletal phenocrysts found in both dacites exhibit normal, reverse, and more commonly oscillatory zoning, which ranges from An_{60} to An_{30}. These large phenocrysts commonly display uncorroded overgrowths which are notably enriched in potassium.

Table 4. Average microprobe analyses of feldspar

Rhyolite

	Plagioclase		Sanidine	
	LV82-19	LV82-28	LV82-19	LV82-28
Wt. % oxides				
CaO	3.65	3.82	0.36	0.41
Na_2O	8.42	8.50	4.98	5.24
K_2O	1.70	1.63	9.56	9.16
Sum	13.77	13.95	14.90	14.81
Equivalent Wt% endmembers				
An	18.09	18.93	1.79	2.02
Ab	71.22	71.89	42.15	44.33
Or	10.07	9.62	56.49	54.11
Total	99.38	100.44	100.43	100.46
Mol. % endmembers				
An	17.43	18.06	1.74	1.96
Ab	72.86	72.77	43.43	45.60
Or	9.71	9.17	54.83	52.44

Dacite

	LV82-4P	LV82-4M	LV82-41P	LV82-41M
Wt. % oxides				
CaO	8.12	10.79	9.40	10.59
Na_2O	7.02	5.64	6.41	5.85
K_2O	0.67	0.45	0.59	0.51
Sum	15.81	16.88	16.40	16.95
Equivalent Wt.% endmembers				
An	40.29	53.52	46.63	52.52
Ab	59.37	47.75	54.22	49.54
Or	3.93	2.67	3.48	2.98
Total	103.59	103.94	104.33	105.05
Mol.% endmembers				
An	37.61	50.07	43.32	48.57
Ab	58.72	47.43	53.45	48.66
Or	3.67	2.50	3.23	2.76

P represents plagioclase phenocrysts
M represents plagioclase microphenocrsts

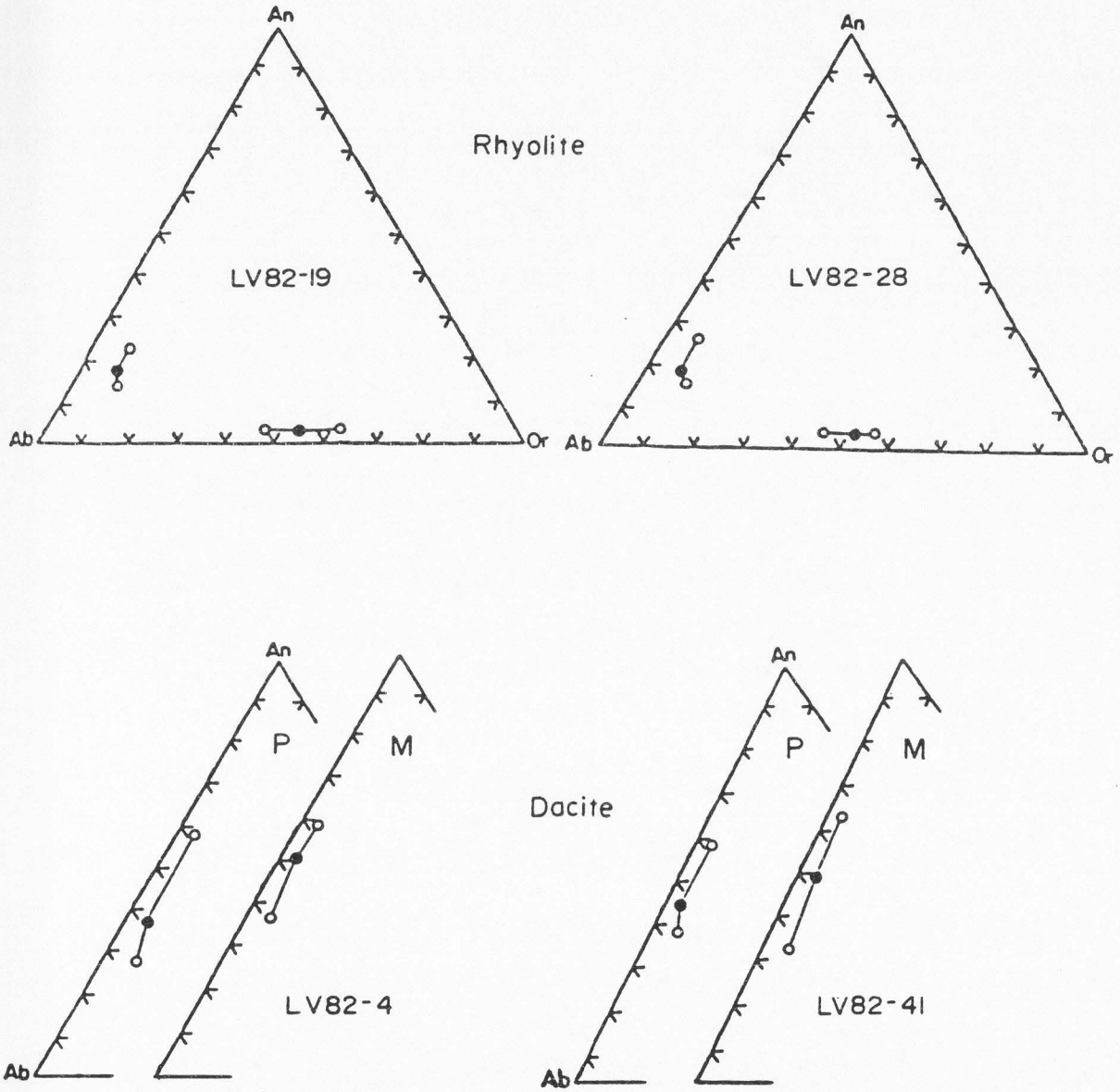

Fig. 2. Electron microprobe analyses of feldspar plotted in terms of mole percent An-Ab-Or. Open circles represent ranges of compositions; filled circles represent average feldspar compositions. P=phenocrysts; M= microphenocrysts.

Euhedral plagioclase microphenocrysts (< 1.0 mm) form a second population, and are zoned from An_{64} to An_{34}. Plagioclase also occurs in all sizes from small microphenocrysts to microlites. The average compositon of the plagioclase microphenocrysts is slightly more calcic than the co-existing larger phenocrysts.

Plagioclase in rhyolitic samples exhibits considerably less compositional zoning than dacitic plagioclase. Anorthite content of the plagioclase phenocrysts ranges from An_{28} to An_{17}.

Sanidine

Average microprobe analyses of sanidine in both rhyolitic samples are presented in Table 4. Sanidine from both samples is zoned, and compositions range from Or_{62} to Or_{47}. Ewart (1979) reported sanidine compositions ranging from Or_{65} to Or_{35} for rhyolites of a bimodal association. The sanidine from the mildly peralkaline rhyolite (LV82-19) is slightly more potassic than sample LV82-28.

Feldspar crystallization

The normative (CIPW) compositions of the representative samples are plotted in terms of their An-Ab-Or components in Fig. 3. Curve EF represents the liquidus field boundary along which liquids coexisting with two feldspars will crystallize (Tuttle and Bowen, 1958). It must be noted that the position of the liquidus curve is a function of pressure, temperature, and Ca content of the liquid (Carmichael et al., 1974). In other two-feldspar, high-K rhyolites

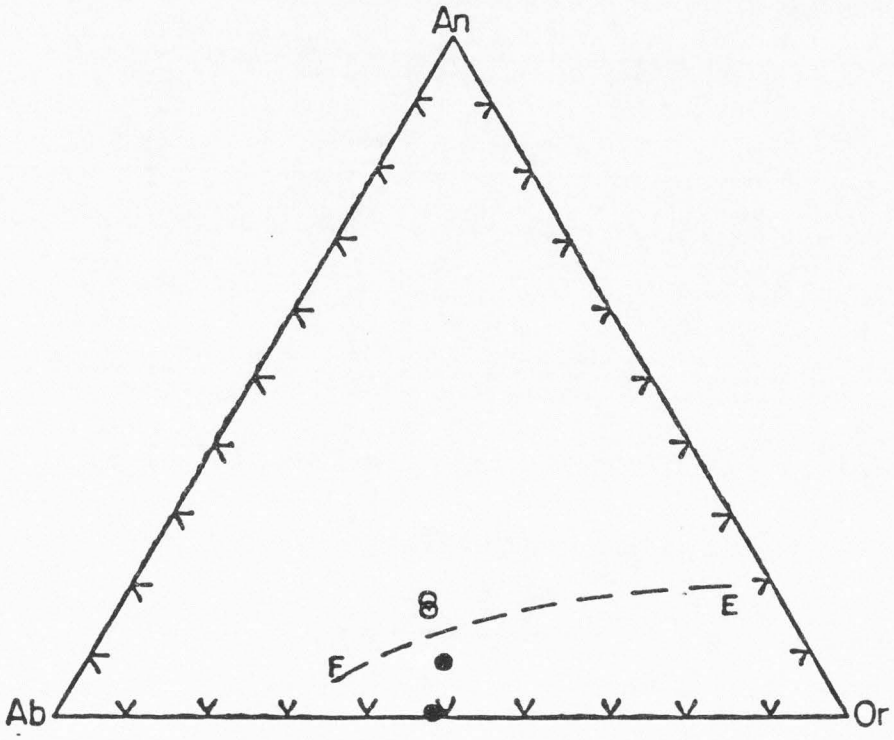

Fig. 3. Normative compositions of study area samples plotted in terms of mole percent An-Ab-Or. Open circles represent dacite samples; filled circles represent rhyolite samples. Line EF represents the two-feldspar liquidus boundary curve. After Tuttle and Bowen (1958).

of a bimodal association, the residual liquid reaches the critical boundary curve at a relatively early stage of the crystallization process (Ewart, 1979). Under ideal equilibrium conditions, the plagioclase will react continuously with the liquid, becoming more sodic until it is completely resorbed, leaving a single homogenous alkali feldspar (Tuttle and Bowen, 1958). The two-feldspar nature of the rhyolites from the study area indicates incomplete resorption of plagioclase phenocrysts. Plagioclase phenocrysts within rhyolite commonly exhibit disequilibrium resorption textures and anhedral crystal outlines supporting the above discussion.

Normative compositions of dacitic samples plot above the liquidus field boundary, indicating plagioclase as the initial feldspar to crystallize (Tuttle and Bowen, 1958). The absence of an alkali feldspar phase in the dacites indicates that the residual liquid did not intersect the liquidus boundary, except possibly at advanced stages of crystallization. The presence of euhedral potassium-rich overgrowths on the large resorbed phenocrysts probably represents a change in liquid composition toward the albite-orthoclase binary minimum during late stages of crystallization (Tuttle and Bowen, 1958).

Amphibole

All dacitic samples from the study area contain amphibole as a major ferromagnesian phenocryst phase. Average microprobe analyses, as well as structural formulas are presented in Table 5.

Both of the dacitic amphiboles contain sufficient aluminum to fill the tetrahedral site, with the excess aluminum occupying octahedral sites. According to Deer et al. (vol. 2, 1963), both samples fall within the calcic amphibole group since the X site is occupied almost exclusively by Ca. Ca also predominates over Na when the X and A sites are considered together.

Leake (1968) has listed criteria on which calcic amphibole analyses may be judged. These include: (a) Si in half unit cell not to exceed 8.08, (b) Si+Al in half unit cell not less than 7.92, and (c) sum of Ca+Na+K in half unit cell must lie between 1.75 to 3.05. Both analyses, on recalculation, fulfill these criteria. In terms of the Leake (1968) classification, the two dacitic amphiboles analyzed are edenitic hornblende.

The amphibole analyses were also evaluated by comparing the number of tetrahedrally coordinated aluminum atoms per formula unit (Fig. 4). Due to the inability of the microprobe to distinguish ferric from ferrous iron, the formula is bracketed using two recalculations. This method, introduced by Stout (1972), involves the calculation of the maximum Fe^{+3}/Fe^{+2} ratio based on 13 cations, and a minimum Fe^{+3}/Fe^{+2} ratio based on 15 cations (including or excluding Na). Upon plotting both recalculations on Fig. 4, the

Table 5. Average microprobe analyses of amphibole

		LV82-4		LV82-41	
SiO_2		45.90		45.78	
TiO_2		2.39		2.38	
Al_2O_3		8.16		7.89	
FeO*		15.07		16.37	
MnO		0.29		0.36	
MgO		12.41		11.95	
CaO		11.46		10.91	
Na_2O		1.76		1.97	
K_2O		0.79		0.86	
F		0.63		0.43	
Cl		0.05		0.07	
O≡F,Cl		0.28		0.20	
Total Wt.%		98.63		98.77	
	Number of Atoms Based on 24 Oxygens				
Si	Z	6.78	8.00	6.79	8.00
Al^{IV}		1.22		1.21	
Al^{VI}		0.20		0.17	
Ti		0.27		0.26	
Fe	Y	1.86	5.10	2.03	5.15
Mn		0.04		0.05	
Mg		2.73		2.64	
Ca		1.81		1.73	
Na	X	0.50	2.46	0.57	2.46
K		0.15		0.16	

*Total iron reported as FeO

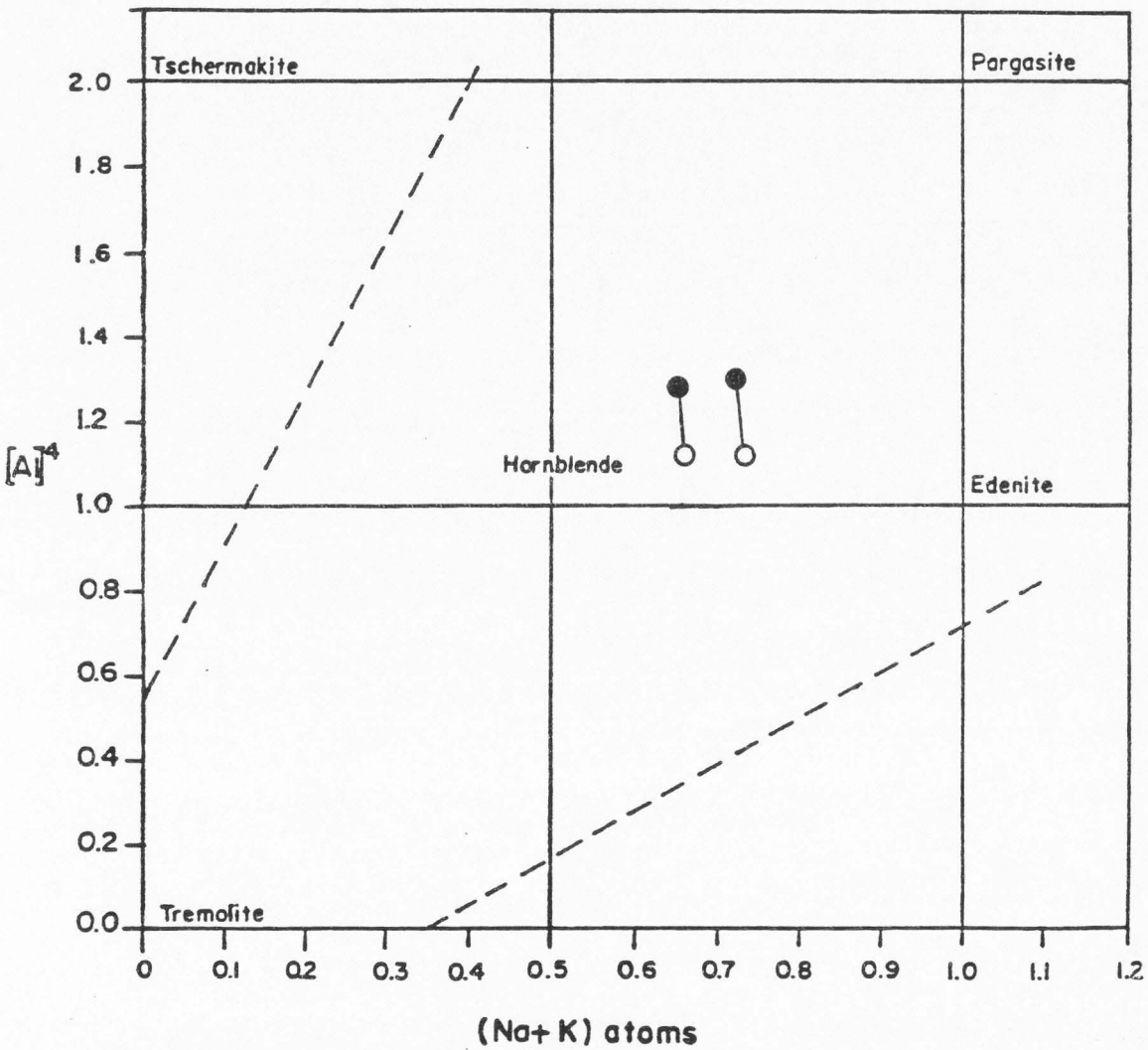

Fig. 4. Average microprobe analyses of hornblende phenocrysts in dacitic samples. Open circles represent tetrahedral Al plotted against A-site occupancy on the basis of normalization to 15 cations. Filled circles represent normalization to 13 cations. After Deer et al., vol. 2 (1963).

dacitic amphiboles lie within the hornblende field.

Hornblendes from the study area commonly exhibit an intense yellow to brown pleochroism, indicating oxidation of common hornblende to oxyhornblende following eruption during the later stages of the consolidation of the lava (Deer et al., vol. 2, 1963).

Biotite

Biotite phenocrysts are present as a major mafic phase in dacite, but occur only as an accessory mineral in rhyolite. Average microprobe analyses and structural formulas for biotites from the two dacitic samples are presented in Table 6. Biotites within rhyolite were not analyzed due to their scarcity and degree of oxidation.

In Fig. 5, the analyses are represented in an FeO-MgO-Al_2O_3 plot, enabling comparison of the present data with that of Nockolds (1947) and Ewart (1971). Both biotite analyses from the study area samples plot within the field delineated by Nockolds (1947) for biotites from calc-alkalic rocks which are associated with hornblende. Both of the analyzed biotites coexist with calcic hornblende and a magnesium-rich orthopyroxene.

Some of the ignimbrites and rhyolitic flows of the Central Volcanic Region of New Zealand studied by Ewart (1971), exhibit ferromagnesian assemblages similar to those of the study area. Biotites from the study area are chemically very similar to those analyzed by Ewart (1971) also coexisting with calcic hornblende and an orthopyroxene. The total value of the Y site occupancy for

Table 6. Average microprobe analyses of biotite

		LV82-4		LV82-41	
SiO_2		37.22		38.04	
TiO_2		4.69		4.96	
Al_2O_3		14.73		14.53	
FeO*		22.31		23.42	
MnO		0.16		0.17	
MgO		10.43		10.44	
CaO		0.03		0.04	
Na_2O		0.84		0.80	
K_2O		8.26		8.18	
F		0.93		0.93	
Cl		0.21		0.20	
O≡F,Cl		0.44		0.43	
Total Wt.%		99.37		101.28	
Number of Atoms Based on 24 Oxygens					
Si	Z	5.53	8.00	5.56	8.00
Al^{IV}		2.47		2.44	
Al^{IV}		0.11		0.06	
Ti		0.53		0.55	
Fe	Y	2.77	5.74	2.86	5.76
Mn		0.02		0.02	
Mg		2.31		2.27	
Ca		-		0.01	
Na	X	0.24	1.81	0.23	1.76
K		1.57		1.52	

*Total iron reported as FeO

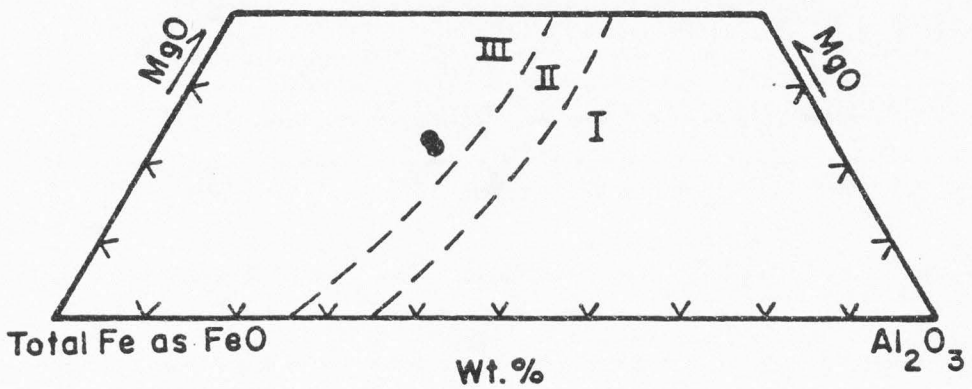

Fig. 5. Average microprobe analyses of biotite phenocrysts in dacitic samples. The area delineated as I corresponds to the compositional field of biotites associated with muscovites. Field II corresponds to biotites unaccompanied by other mafic minerals. Field III corresponds to biotites associated with hornblende, pyroxene, or olivine. After Nockolds (1947).

samples LV82-4 and LV82-41 is 5.74 and 5.76, respectively, and corresponds closely to the average value of 5.85 reported by Nockolds (1947) for biotites coexisting with hornblende.

Pyroxene

Orthopyroxene is present as a common phenocryst phase in both of the dacite vitrophyres analyzed. Coexisting clinopyroxenes were not found in any of the dacitic samples studied. Results of average microprobe analyses, along with structural formulas are presented in Table 7. The enstatite-ferrosilite-wollastonite projection of the analyses for both samples is presented in Fig. 6.

The orthopyroxene phenocrysts lie in the hypersthene to ferrohypersthene field. LV82-4 shows the largest compositional range from $En_{67}Fs_{33}$ to $En_{45}Fs_{55}$, with an average composition of $En_{60}Fs_{40}$. LV82-41 is slightly more magnesium rich, with an average composition of $En_{64}Fs_{36}$. The variability observed occurs primarily between individual grains rather than within them. The dacitic orthopyroxenes from the study area are chemically very similar to those found in dacites directly north, in the areas studied by Olesen (Utah State Univ., pers. comm.) and Hare (1982).

The Ca atoms (per formula unit) for LV82-4 and LV82-41 are both 0.048. These values correspond closely to the values reported by Kuno (1954) and Ewart (1971) for dacitic orthopyroxenes coexisting with hornblende. These orthopyroxenes are also considerably richer in Mn than their associated biotite or hornblende.

Table 7. Average microprobe analyses of pyroxene

	LV82-4		LV82-41	
SiO_2	52.72		54.29	
TiO_2	0.16		0.19	
Al_2O_3	1.38		1.15	
FeO*	24.73		21.77	
MnO	0.91		0.72	
MgO	19.28		21.31	
CaO	1.20		1.22	
Na_2O	0.16		0.15	
Total Wt.%	100.54		100.80	
	Number of Atoms Based on 6 Oxygens			
Si	1.9801	2.0000	1.9993	2.0000
Al^{IV}	0.0199		0.0007	
Al^{VI}	0.0412		0.0492	
Ti	0.0045		0.0053	
Fe	0.7768	1.9307	0.6705	1.9172
Mn	0.0289		0.0225	
Mg	1.0793		1.1697	
Ca	0.0483	0.0600	0.0481	0.0588
Na	0.0117		0.0107	

*Total iron reported as FeO

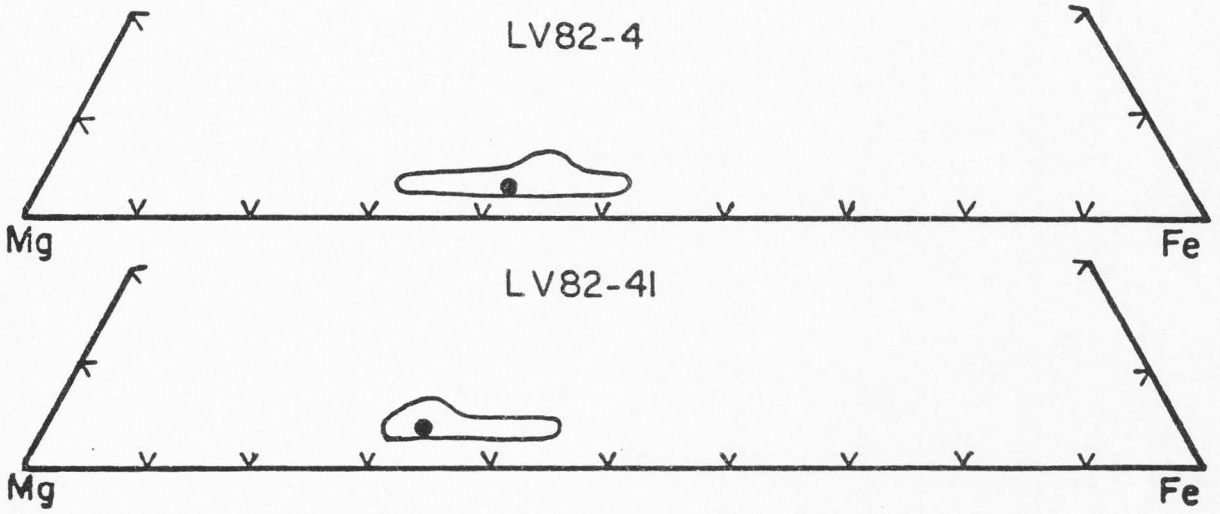

Fig. 6. Average microprobe analyses of orthopyroxene phenocrysts in dacitic samples. Data plotted in terms of mole percent endmembers: wollastonite (Ca), enstatite (Mg), ferrosilite (Fe). Filled circles represent the average analysis for each sample.

Iron-Titanium Oxides

Average microprobe analyses of coexisting titanomagnetite and ilmenite from both dacitic samples are presented in Table 8. Iron-titanium oxides within the rhyolitic samples were oxidized or exsolved, preventing microprobe analyses. Table 8 also presents equilibrium temperatures and oxygen fugacities derived using equations from Powell and Powell (1977).

Ulvospinel content in the titanomagnetite from samples LV82-4 and LV82-41 is 37.03 and 37.04 mole percent, respectively, as calculated according to the method of Carmichael (1967). Ilmenite values are 7.13 and 7.40 mole percent R_2O_3, respectively.

Fe_2O_3 has been determined using the method of Carmichael (1967), wherein sufficient FeO is allotted to the ulvospinel structure to satisfy its stoichiometric needs, with the excess FeO recalculated to equivalent magnetite. Fe_2O_3 is recalculated in a similar manner for ilmenite.

Table 8. Average microprobe analyses of coexisting Fe-Ti oxides (Wt. %)

	Magnetite		Ilmenite	
	LV82-4	LV82-41	LV82-4	LV82-41
SiO_2	2.38	2.78	2.11	2.18
TiO_2	10.02	9.75	46.98	47.39
Al_2O_3	2.10	2.03	0.35	0.39
V_2O_3	0.38	0.42	0.00	0.00
Cr_2O_3	0.15	0.11	0.00	0.00
FeO*	79.27	81.36	48.31	49.10
MnO	0.42	0.35	0.88	0.81
MgO	0.34	0.26	1.05	1.03
NiO	<0.05	<0.05	<0.03	<0.03
CaO	0.09	0.08	0.04	0.05
ZnO	0.29	0.16	0.00	0.06
Sum	95.49	97.35	99.75	101.04
Fe_2O_3**	40.95	41.94	7.09	7.42
FeO	42.42	43.63	41.93	42.42
Total	99.59	101.55	100.46	101.78
Mol% Usp	37.03	37.04		
R_2O_3			7.13	7.40
T (°C)	788	793		
-Log f_{O_2}	14.55	14.37		

*Total iron reported as FeO
**Recalculated from FeO using method of Carmichael (1967).

CHEMISTRY

Major Elements

Chemical analyses of the representative samples are presented in Table 9, along with C.I.P.W. norms calculated on an anhydrous basis. On the basis of a simple plot of weight percent SiO_2 versus K_2O used by Ewart (1979), both rhyolites are classified as high-K rhyolite and both dacites as high-K dacite. In this classification rhyolite has greater than 70 weight percent silica, and dacite has 63 to 69 weight percent silica.

In rhyolitic samples, SiO_2 exhibits the largest range of the major oxides. SiO_2 values are 75.38 in sample LV82-28 and 77.09 in sample LV82-19. Of particular interest is the difference in alumina saturation between the two rhyolitic samples. Sample LV82-28 is a metaluminous, high-silica rhyolite with Al_2O_3 (mole proportion) less than $[CaO+K_2O+Na_2O]$, but exceeding $[Na_2O+K_2O]$, while sample LV82-19 is a mildly peralkaline, high-silica rhyolite with Al_2O_3 slightly less than $[Na_2O+K_2O]$ (Carmichael et al., 1974).
The peralkaline nature of LV82-19 results in the presence of the sodic pyroxene, acmite, in the norm. The lower silica rhyolite contains almost twice the amount of CaO, but this is not reflected by modal or compositional variations in plagioclase (see Table 3 and Fig. 7).

The dacitic samples represented by two vitrophyres are virtually indistinguishable from one another by their major-element chemistry and possibly represent a single eruptive unit. Silica

Table 9. Major element analyses and C.I.P.W. norms of representative samples

	Dacite				Rhyolite	
	LV82-4	LV82-4G*	LV82-41	LV82-41G*	LV82-19	LV82-28
SiO_2	69.31	74.87	69.41	74.05	77.09	75.38
TiO_2	0.34	0.12	0.33	0.12	0.21	0.10
Al_2O_3	14.21	12.58	14.25	12.29	11.10	12.66
Fe_2O_3	1.18	--	1.15	--	1.40	1.33
FeO	1.20	1.92	1.24	1.80	0.00	0.05
MnO	0.03	0.02	0.05	0.02	0.03	0.02
MgO	0.76	0.06	0.76	0.08	0.00	0.00
CaO	2.30	0.74	2.29	0.72	0.64	1.47
Na_2O	3.10	2.60	3.03	2.76	3.72	3.32
K_2O	4.28	4.89	4.29	4.96	5.06	4.75
P_2O_5	0.15	--	0.14	--	0.07	0.04
H_2O+	2.41	--	2.73	--	0.40	0.51
H_2O-	0.40	--	0.41	--	0.06	0.10
Total	99.67	97.80	100.08	96.80	99.78	99.73
Q	28.93	37.82	29.32	35.92	36.08	35.16
C	0.66	1.67	0.79	1.07	--	--
or	25.29	28.90	25.35	29.31	29.90	28.07
ab	26.23	22.00	25.64	23.35	28.93	28.09
an	10.43	3.67	10.45	3.57	--	5.59
ac	--	--	--	--	2.25	--
wo	--	--	--	--	0.88	0.57
hy-en	1.89	0.15	1.89	0.20	--	--
hy-fs	0.72	3.36	0.87	3.14	--	--
mt	1.71	--	1.67	--	--	--
il	0.65	0.23	0.63	0.23	0.06	0.15
hm	--	--	--	--	0.62	1.33
tn	--	--	--	--	0.43	0.05
ap	0.36	--	0.33	--	0.17	0.09
Total	96.87	97.80	96.94	96.79	99.32	99.10
Femic	5.33	3.74	5.39	3.57	4.41	2.20
Salic	91.54	94.06	91.55	93.22	94.91	96.90

* glass analyzed by microprobe; total Fe reported as FeO
Values reported in Wt.%

content shows very little variation with values of 69.31 and 69.41 weight percent. Both samples are peraluminous, with (mole proportion) $Al_2O_3 > (Na_2O+K_2O+CaO)$, and corundum normative. The high water content of both dacitic samples reflects the hydrated nature of the glassy groundmass. Comparison of the dacite whole-rock analyses with analyses of their residual glasses shows the residual glasses to be higher in SiO_2 and K_2O and lower in Al_2O_3, MgO, CaO, and TiO_2.

Figure 7 is a plot of the major oxides in rhyolitic and dacitic samples versus their corresponding silica contents. The similarity of the dacitic samples is indicated by the lack of variation in the major oxides. The data for the rhyolite samples indicate some differences in major-element chemistry between LV82-19 and LV82-28. The higher silica rhyolite (LV82-19) contains more K_2O and Na_2O, and less Al_2O_3 and CaO. Total Fe and MgO contents for the rhyolites are very similar.

Fig. 8 shows the normative compositions of the representative samples in the system $NaAlSi_3O_8$-$KAlSi_3O_8$-SiO_2-H_2O projected to the anhydrous base. Both the rhyolitic and dacitic samples plot very close to the "ternary" minimum for a confining pressure of 1000 bars. If this value is considered an estimate of pre-eruption water-vapor pressure, then the temperature of an ideal rhyolite in equilibrium with phenocrysts of quartz and feldspar is about 730 degrees Celsius, and the equilibrium water content is about 4.6 percent (Tuttle and Bowen, 1958). Although no alternate methods of estimating equilibrium water pressures and temperatures are

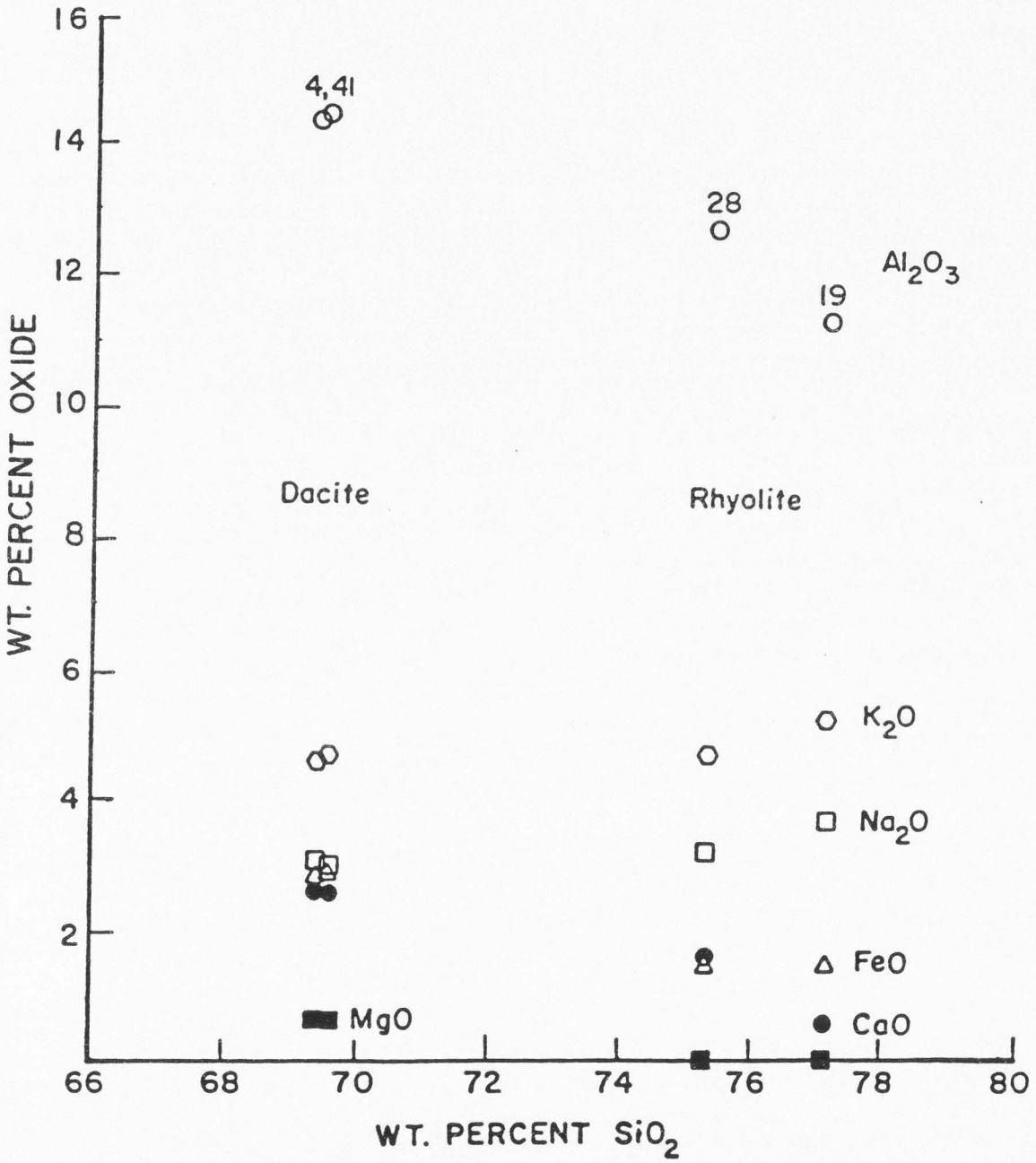

Fig. 7. Variation diagram (Harker type) for volcanic rocks of the study area. Total Fe expressed as FeO.

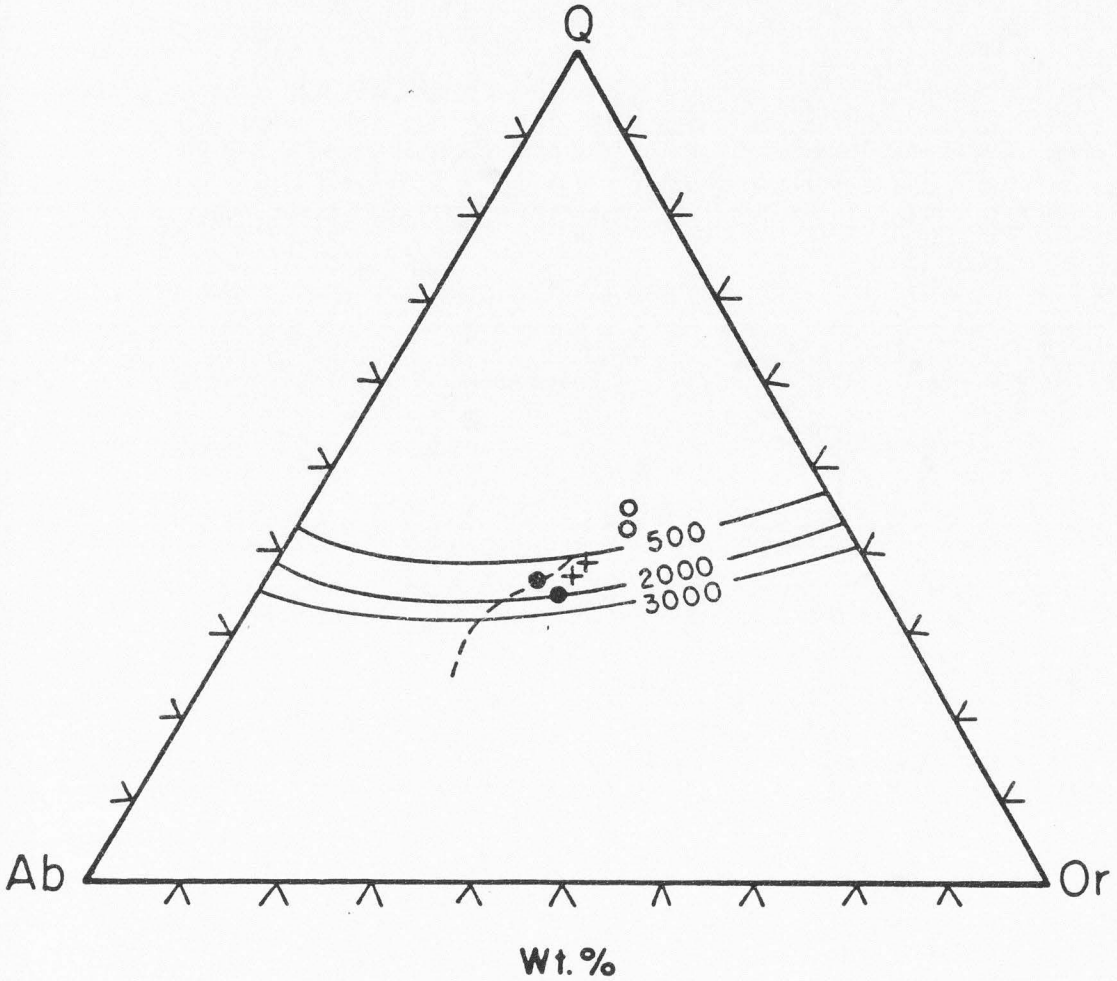

Fig. 8. Normative compositions of study area samples plotted with respect to the system Q-Ab-Or. Crosses represent rhyolitic samples; filled circles represent dacitic samples; open circles represent residual dacitic glass. Solid lines represent boundary curves between quartz and feldspar at various water pressures. Dashed line represents path of isobaric minima. After Tuttle and Bowen (1958).

available for the rhyolites, the high water content is consistent with the presence of two phenocrystic feldspars in both rhyolites (Tuttle and Bowen, 1958). The displacement of the residual dacitic glasses away from the Ab apex could be explained by loss of Na^{+} and gain of K^{+}, H^{+}, and Ca^{++} during an exchange with natural waters (Truesdell, 1966).

Trace Elements

The same four samples from the study area that were analyzed for major elements, along with two rhyolites and one dacite from the Rhyolite Mountains were analyzed for twelve trace elements by X-ray fluorescence. The results are presented in Table 10 and 11. In Fig. 9, trace-element concentrations are plotted against Rb, an incompatible element used here as a monitor of magmatic evolution. The plots show that Zr, Sr, and Ba systematically decrease with increasing Rb, whereas Y and Nb generally increase.

The rhyolites have distinctive trace-element abundance patterns relative to dacites, notably the extreme depletion of Sr and Ba, and enrichment of Nb and Rb. The high Rb content in both rhyolites is expected in rocks with high alkali content. Although sample LV82-19 would be expected to contain a higher Rb concentration than LV82-28, the opposite is observed. This unexpected difference can be attributed to a statistical counting error in the XRF analyses. The mildly peralkaline rhyolite (LV82-19) can be distinguished from the metaluminous rhyolite (LV82-28) by a relative enrichment of the more highly charged cations (e.g., LREE, Zr, and Y). The strong

Table 10. Trace element analyses of representative samples

	Dacite			Rhyolite		
	LV82-4	LV82-41	TCV82-55	LV82-19	LV82-28	TCV82
Ti	2255	2237	2454	587	548	484
Ba	1164	1326	1118	109	120	24
Nb	19	20	22	41	44	31
Zr	157	221	229	154	146	123
Y	32	41	39	117	71	45
Sr	232	231	189	19	24	10
Rb	80	80	104	175	184	238
Zn	47	47	50	43	45	31
La	84	77	82	74	64	46
Ce	153	171	167	141	131	84
Pr	20	22	18	22	20	8
Nd	55	65	56	90	48	33

All trace elements determined by X-ray fluorescence in ppm

a.

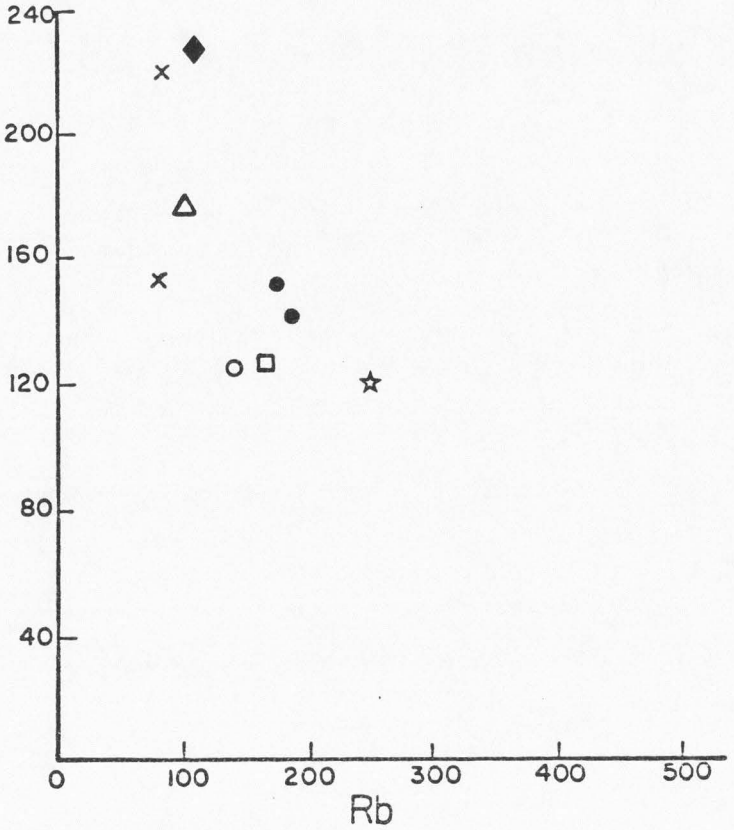
240
200
160
Zr
120
80
40
0
100
200
300
400
500
Rb

b.

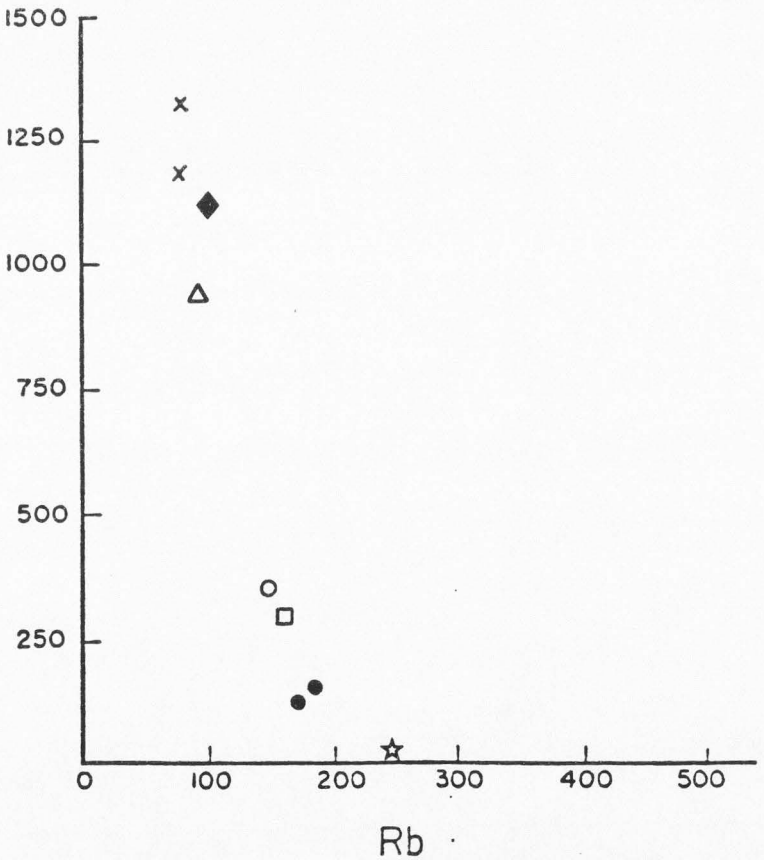
1500
1250
1000
Ba
750
500
250
0
100
200
300
400
500
Rb

c. Nb

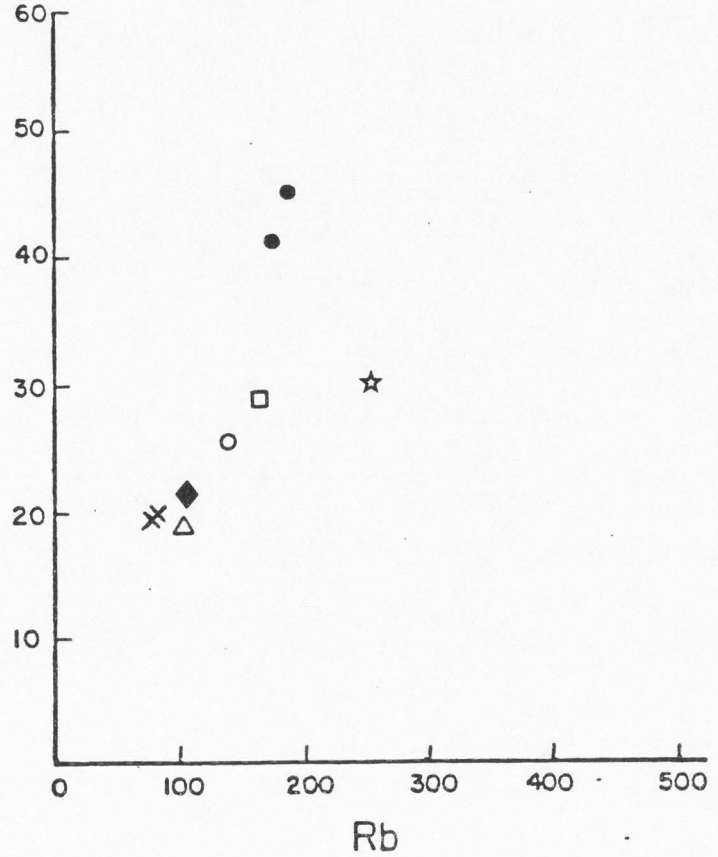
60
50
40
30
20
10
0
100
200
300
400
500
Rb

d. Ce

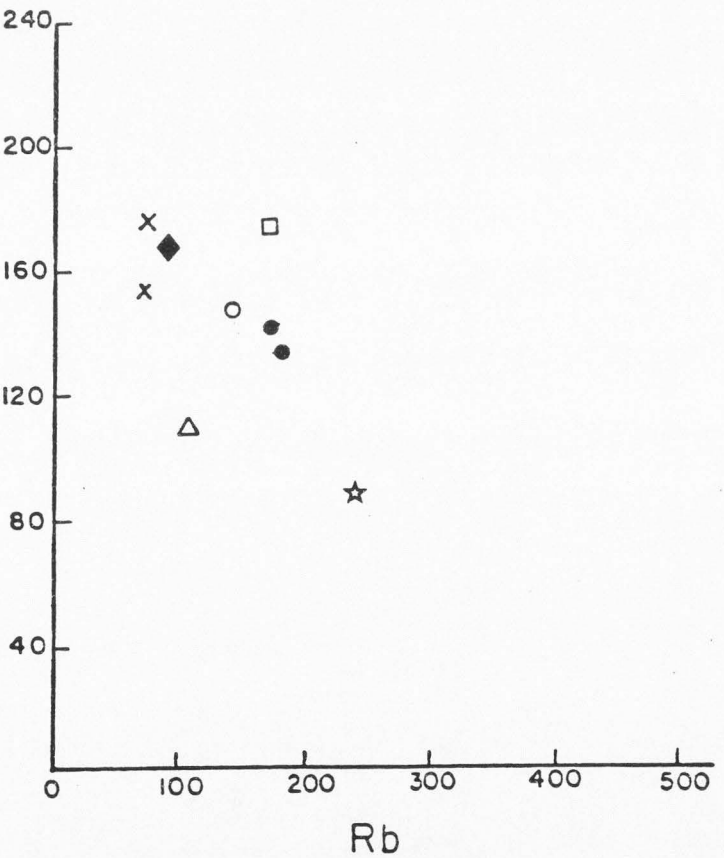
240
200
160
120
80
40
0
100
200
300
400
500
Rb

e. Sr

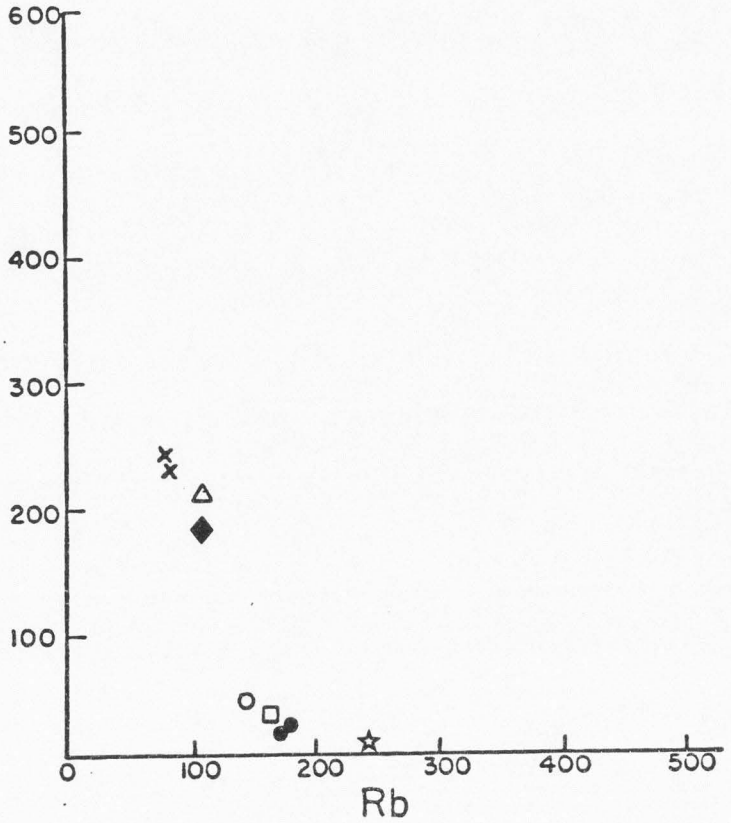
600
500
400
300
200
100
0
100
200
300
400
500
Rb

f. Y

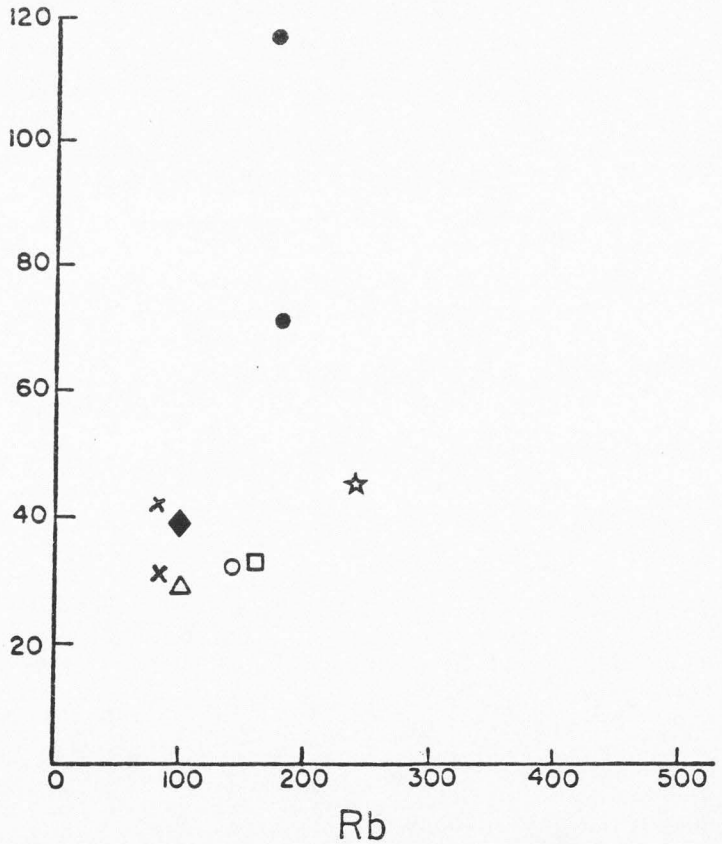
120
100
80
60
40
20
0
100
200
300
400
500
Rb

depletion of Sr and Ba in rhyolite, can in principle be explained by fractionation of feldspars. Rb/Sr ratios increase from 0.35 at 69% SiO_2 to 9.0 at 77% SiO_2.

The trace element patterns of the two dacitic samples are very similar, corresponding to their near identical major-element compositions. Although no direct stratigraphic relation can be determined between sample LV82-4 and LV82-41, the chemical similarity between the two indicates little primary chemical variation within single cooling units.

Comparative Analyses

Table 11 presents major- and trace-element analyses of selected rhyolites and dacites from other areas. All of the selected samples are high-K varieties from bimodal associations in the western United States. Both Ewart (1979) and Christiansen and Lipman (1972) compiled major- and trace-elememt data for salic volcanics from several areas characterized by a bimodal association. Chemically these rhyolites are high silica, low Ca + Mg, and high alkali rocks. The two rhyolites of the study area generally contain higher amounts of titanium relative to rhyolites with similar silica contents, otherwise, they exhibit similar major element chemistries. The two dacites of the study area also have very similar chemistries compared with the selected samples, except they contain a lesser amount of total iron than the average high-K dacites from the western United States (Ewart, 1979).

The trace element patterns of the study area samples are very

Table 11. Major- and trace-element analyses of selected samples

Wt.%	1	2	3	4	5	6	7
SiO_2	77.60	77.88	75.00	75.26	75.75	67.52	69.23
TiO_2	0.09	0.12	0.06	0.06	0.18	0.55	0.33
Al_2O_3	10.97	11.74	12.21	13.05	13.08	16.21	14.02
Fe_2O_3	1.14	0.50	0.45	0.89	1.02	2.61	1.38
FeO	0.11	0.57	0.53	0.08	0.40	0.83	1.26
MnO	0.01	0.01	0.01	0.06	0.06	0.09	0.03
MgO	0.22	0.05	0.01	0.08	0.23	0.90	0.49
CaO	0.74	0.77	0.02	0.72	0.67	2.63	2.79
Na_2O	3.27	3.01	4.32	3.96	3.67	4.07	3.24
K_2O	4.67	5.06	4.25	5.26	4.89	4.39	3.94
P_2O_5	0.03	0.02	0.01	0.08	0.04	0.19	0.09
H_2O+	0.55	0.24	2.44	0.09	-	-	2.71
H_2O-	0.07	0.05	0.22	0.02	-	-	0.44
Total	100.68	100.12	99.53	99.72	99.99	99.99	99.95

1.) Domal Rhyolite, Rhyolite Mts., Ut. (Smith, 1980, Table 9,#9-4-1)
2.) Rhyolite, Rhyolite Mts., Ut. (Hare, 1982, Table 6, DV80-1)
3.) Rhyolite vitrophyre, Coso Field, Ca. (Bacon et al,1981, Table 1a)
4.) Rhyolite. Twin Peaks. Ut., (Crecraft et al.,1981,Table 4,no.2)
5.) Rhyolite, Western USA (average), (Ewart,1979,Appendix 3a)
6.) High-K dacite, Western USA (average), (Ewart,1979,Appendix 3a)
7.) Dacite vitrophyre, Rhyolite Mts., Ut. (Hare,1982,Table 6,no.1)

ppm	1*	2*	3	4	5	6	7*
Ti	765	778	n.d.	550	n.d.	n.d.	1978
Ba	344	266	n.d.	16	409	1680	925
Nb	26	29	72	34	36	19	19
Zr	123	125	100	95	172	246	173
Y	33	35	74	42	29	31	27
Sr	47	32	n.d.	21	118	538	208
Rb	147	171	315	259	231	93	108
Zn	23	30	53	36	n.d.	68	46
La	64	80	16	17	75	88	68
Ce	132	153	39	46	100	271	105
Pr	17	15	n.d.	n.d.	n.d.	n.d.	13
Nd	55	59	22	24	n.d.	n.d.	46

* determined with XRF by Bruce Scarbrough

similar to other rhyolites and dacites from the Rhyolite Mts. (Table 11, # 1,2,5, and Fig. 9). The rhyolites of the study area are depleted in Ba, Rb, Zr, and Sr relative to an average value for high-K rhyolites (Table 11, #7), and enriched in Ce and Y. Like other bimodal rhyolites, the strong depletion of Sr, Ba, and ferromagnesian elements such as Mg and Mn, indicate a control by crystal fractionation, at least in the latter stages of development (Ewart, 1979).

PETROGENESIS

The overall similarities in mineralogy and major- and trace-element chemistry suggest that the volcanic rocks within the Rhyolite Mts. are genetically related. A small volume of Tertiary basalt dated at 16.3 m.y.b.p. (Armstrong et al., 1976) is located approximately 4 miles northwest of the study area and supports the bimodal nature of the volcanism by both its occurrence and age. By analogy with other "bimodal" volcanic fields in the western United States, it is assumed that the silicic magmas within the Rhyolite Mts. are products of partial melting of crustal rocks, brought upon principally by intrusion of mafic magma from the mantle (Lachenbruch, 1978/1979). The extent to which these magmas have been modified during their ascent is difficult to assess, yet certain constraints can be placed on the possible mechanisms respondsible.

Hildreth (1979) looked at a sequence of silicic tuffs which erupted from a compositionally zoned magma chamber and which reflected the chemical variations within a source magma chamber at one point in time. Although limited, radiometric age dating indicates that a considerable age difference exists between dacitic and rhyolitic eruptive units in the study area, and therefore, the chemical elemental patterns observed are assumed to have evolved with time.

The mechanism which would most likely account for the transition from dacitic to rhyolitic volcanism in the study area is

fractional crystallization of a dacitic liquid to produce a rhyolitic liquid. The dacitic liquid could be derived by fractional crystallization of a more mafic liquid or possibly it represents a direct product of crustal fusion. The simplest crystal fractionation model involves fractionating the dacite to produce a rhyolite. In order to test this hypothesis, a least squares, mass-balance, magmatic differentiation model (Stormer and Nicholls, 1978) was used to calculate the proportions of phases that must be subtracted from a parent magma to produce a daughter magma. Table 12 presents the results of this differentiation model. Dacite sample LV82-41 (69% SiO_2) was used for the parent magma, and rhyolite sample LV82-28 (75% SiO_2) was used as a daughter magma. Microprobe analyses of phenocrysts in dacite were utilized to estimate the amounts of fractionated phases. Calculations show that fractionation of plagioclase along with minor orthopyroxene and magnetite from LV82-41 will produce a melt similar in composition to LV82-28. The relative proportions of the fractionated minerals are similar to the actual proportions of minerals found in the parent rock. Although a good solution was obtained, this only suggests that a common process such as fractional crystallization of a parent magma could account for the observed rhyolite occurrence. Other chemical patterns suggesting crystal fractionation as the dominant differentiation process include: (1) decrease in Sr accompanying increasing SiO_2 indicating feldspar fractionation, and (2) decreasing P_2O_5 and Zr with increasing SiO_2, indicating separation of apatite and zircon, both of which are common accessories.

Table 12. Results of least square differentiation model

Differentiating from LV82-41 to LV82-28		
Phase Name	Amount subtracted from initial magma (wt%)	Sum of the squares of the residuals
Plagioclase (An_{43})	15.37	
Orthopyroxene (En_{64})	3.18	0.6740
Magnetite (Mt_{63})	0.85	
Total	19.40	

Incremental partial melting of a common crustal source could explain the occurrence of rhyolitic volcanism prior to dacitic volcanism, and also represent the source of a dacitic liquid which was later fractionated to produce the younger rhyolite. Initial partial melts would be enriched in Si and Rb and depleted in Fe, Mg, and Ti relative to subsequent melt fractions. Complexities of trace-element behavior and lack of data on source rocks preclude more rigorous evaluation of partial melting. The lack of Sr isotope data prevents delineating the source region in terms of upper or lower crustal origin and amount of crustal assimilation. Geobarometric studies on the rhyolite domes located at the north end of the Rhyolite Mts. show depths of equilibration of phenocrysts with liquid ranging from 18.2 to 0.4 km (Smith, 1980). If similar equilibration depths are inferred for similar rocks in the study area, an upper crustal source is likely. Fractional crystallization of the dacitic liquid must have taken place in the crust where plagioclase, pyroxene, and hornblende are stable. In summary, the transition from dacitic to younger rhyolitic volcanism in the southern portion of the study area seems to result from crystal fractionation in shallow magma chambers.

CONCLUSION

The assemblage of silicic volcanic rocks within the study area and the Rhyolite Mts. as a whole represents the silicic endmembers of a bimodal basalt-rhyolite association. This style of Basin and Range volcanism was dominant starting approximately 15 million years ago, and represents the second stage of Basin and Range volcanism (Smith, 1977). Age dating of samples from the study area and other parts of the Rhyolite Mts. supports this observation and indicates that silicic volcanism was episodic and took place between 13.0 and 8.0 m.y. ago.

The dacite and rhyolite of the study area are chemically very similar to other dacites and rhyolites analyzed from the Rhyolite Mts. and also to other high-silica dacites and rhyolites found associated with basalt in the western United States. The trace element patterns are also very characteristic of those observed in high-K rhyolites and dacites of the western United States.

The transition from dacitic to rhyolitic volcanism observed in the southern portion of the study area seems to represent a time period of approximately 4 to 5 million years. Disregarding the possible effects of wall rock interaction, the chemical variations between these two rocks evolved over time and apparently are a result of differentiation of a common magma or similar parent magmas. The mineralogical and overall geochemical characteristics indicate the dominant mechanism in the differentiation process was crystal fractionation in relatively shallow magma chambers.

The linear distribution of the volcanic rocks composing the Rhyolite Mts. suggests that the volcanism was strongly fault controlled, and probably resulted from the propagation of silicic dike-like bodies through elongate subsurface conduits. The magmas were emplaced passively through multiple sites commonly characterized by a fissure-type vent geometry. The extensional nature of the Great Basin during the late Tertiary facilitated the formation of these subsurface conduits.

REFERENCES

Albee, A. L., and Ray, L., 1970, Correction factors for electron probe microanalysis of silicates, carbonates, phosphates, and sulphates: Anal. Chem., v. 42, p. 1408-1414.

Armstrong, R. L., Speed, R. C., Graustein, W. C., and Young, A. Y., 1976, K-Ar dates from Arizona, Montana, Nevada, Utah, and Wyoming: Isochron/West, v. 16, p. 1-6.

Bacon, C.R., Macdonald, R., Smith, R. L., and Baedecker, P. A., 1981, Pleistocene high-silica rhyolites of the Coso volcanic field, Inyo County, California: Journal of Geophysical Research, v. 86, p. 10223-10241.

Barnes, V. E., 1930, Changes in hornblende at about 800 C: American Mineralogist, v. 15, p. 393.

Bence, A. E., and Albee, A. L., 1968, Empirical correction factors for the electron microanalysis of silicates and oxides: Journal of Geology, v. 76, p. 382-403.

Carmichael, I. S. E., 1967, The iron-titanium oxides of salic volcanic rocks and their associated ferromagnesian silicates: Contributions to Mineralogy and Petrology, v. 14, p. 36-64.

Carmichael, I. S. E., Turner, F. J., and Verhoogen, J., 1974, Igneous Petrology: N.Y., McGraw-Hill, 739 p.

Christiansen, R. L., and Lipman, P. W., 1966, Emplacement and thermal history of a rhyolite lava flow near Fortymile Canyon, southern Nevada: Geological Society of America Bulletin, v. 77, p. 671-684.

Christiansen, R. L., and Lipman, P. W., 1972, Cenozoic volcanism and plate tectonic evolution of the western United States, Pt. II, Late Cenozoic: Philosophical Transactions of the Royal Society of London, A. 271, p. 249-284.

Compton, R. R., Todd, V. R., Zartman, R. E., and Naeser, C. W., 1977, Oligocene and Miocene metamorphism, folding, and low-angle faulting in northwestern Utah: Geological Society of America Bulletin, v. 88, p. 1237-1250.

Crecraft, H. R., Nash, W. P., and Evans, S. H., Jr., 1981, Late Cenozoic volcanism at Twin Peaks, Utah: geology and petrology: Journal of Geophysical Research, v. 86, p. 10303-10320.

Deer, W. A., Howie, R. A., and Zussman, J., 1963, Rock forming minerals , v. 1-5, N.Y., Wiley and Sons, Inc.

Delaney, P. T., and Pollard, D. D., 1981, Deformation of host rocks and flow of magma during growth of minette dikes and breccia-bearing intrusions near Ship Rock, New Mexico: U.S.G.S. Prof. Paper 1202, 61 p.

Doelling, H. H., 1980, Geology and mineral resources of Box Elder County, Utah: Utah Geological and Mineral Survey Bulletin 115, 251 p.

Ewart, A., 1971, Notes on the chemistry of ferromagnesium phenocrysts from selected volcanic rocks, Central Volcanic Region: New Zealand Journal of Geology and Geophysics, v. 14, p. 323-340.

Ewart, A., 1979, A review of the mineralogy and chemistry of Tertiary-Recent dacitic, latitic, rhyolitic, and related salic volcanic rocks: in F. Barker, editor, Developments in Petrology: Trondjhemites, Dacites, and Related Rocks, N.Y., Elsevier Scientific Publishing Co., p. 13-121.

Fenneman, N. M., and Johnson, D. W., 1946, Physical divisions of the United States: U.S. Geological Survery Map, Scale 1:7,000,000.

Fink, J. H., and Pollard, D. D., 1983, Structural evidence for dikes beneath silicic domes, Medicine Lake Highland Volcano, Calif.: Geology, v. 11, no. 8, p. 458-461.

Hare, E. M., 1982, Structure and petrography of the Tertiary volcanic rocks between Death Creek and Dairy Valley Creek (Box Elder Co.), Utah: M.S. Thesis, Utah State University, 64 p.

Hildreth, W., 1979, The Bishop Tuff: evidence for the origin of compositonal zonation in silicic magma chambers: in Chapin, C. E., and Elston, W. E., eds., Ash-flow tuffs: Geological Society of America Spec. Paper 180, p. 43-75.

Hood, J. W., and Price, D., 1970, Hydrologic reconnaissance of Grouse Creek Valley, Box Elder Co., Utah: Utah Dept. of Natural Resources Tech. Pub. 29, 54 p.

Kuno, H., 1954, Study of orthopyroxenes from volcanic rocks: American Mineralogist, v. 39, p. 30-46.

Lachenbruch, A. H., 1978/1979, Heat flow in the Basin and Range province and thermal effects of tectonic extension: Pure and Applied Geophysics, v. 117, p. 34-50.

Leake, B. E., 1968, A catalog of analyzed calciferous and subcalciferous amphiboles together with their nomenclature and associated minerals: Geological Society of America Spec. Paper 98, 65 p.

Lofgren, G. E., 1971, Experimentally produced devitrification textures in natural rhyolite glass: Geological Society of America Bulletin, v. 82, p. 111-124.

Lofgren, G. E., 1976, Nucleation and growth of feldspar in dynamic crystallization experiments (abstract): Geological Society of America Abstracts with Programs, v. 8, p.982.

Mapel, W. S., and Hail, W. J., 1956, Tertiary stratigraphy of the Goose Creek District, Idaho and adjacent parts of Utah and Nevada: Utah Geological Sociey Guidebook, no. 11, p. 1-16.

Maxwell, J. A., 1968, Rock and mineral analysis: N.Y., John Wiley and Sons, 584 p.

McKee, E. H., 1971, Tertiary igneous chronology of the Great Basin of the western United States-implications for tectonic models: Geological Society of America Bulletin, v. 82, p. 3497-3502.

Nicholls, J., Fiesinger, D. W., and Ethier, V. G., 1977, Fortran IV programs for processing routine electron microprobe data: Computers and Geosciences, v. 3, p.49-83.

Nobel, D. C., 1972, Some observations on the volcano-tectonic evolution of the Great Basin, western United States: Earth and Planetary Science Letters, v. 17, p. 142-150.

Nockolds, S. R., 1947, The relation between chemical composition and paragenesis in biotite micas of igneous rocks: American Journal of Science, v. 245, p. 400-417.

Parsons, W. H., 1969, Criteria for the recognition of volcanic breccias: Geological Society of America Mem. 115, p 263-301.

Phillips, W. R., and Griffen, D. T., 1981, Optical Mineralogy of the nonopaque minerals: San Francisco, Freeman and Co., 677 p.

Powell, R. and Powell, M., 1977, Geothermometry and oxygen barometry using iron-titanium oxides; a reappraisal: Mineralogical Magazine, v. 41, p. 257-263.

Smith, K. W., 1980, Structure and petrology of Tertiary volcanic rocks near Etna, Utah: M.S. Thesis, Utah State University, 83 p.

Smith, R. B., 1977, Seismicity, crustal structure, and intraplate tectonics of the interior of the western Cordillera, in Smith, R. B., and Eaton, G. P., editors, Cenozoic tectonics and regional geophysics of the western Cordillera: Geological Society of America Mem. 152, p. 111-144.

Smith, R. P., and Nash, W. P., 1976, Chemical correlation of volcanic ash deposits in the Salt Lake Group, Utah, Idaho, and Nevada: Journal of Sedimentary Petrology, v. 46, no. 4, p. 930-939.

Stewart, J. H., 1971, Basin and Range structure: a system of horsts and grabens produced by deep-seated extension: Geological Society of America Bulletin, v. 82, p. 1019-1044.

Stewart, D. B., 1979, The formation of siliceous potassic glassy rocks, in Yoder, H. S., ed., The evolution of the igneous rocks, fiftieth anniversary perspectives: Princeton, Princeton University Press, p. 339-349.

Stokes, W. L., 1963, Geologic map of Utah: Salt Lake City, University of Utah, Scale 1:250,000.

Stormer, J. C., and Nicholls, J., 1978, XLFRAC: A program for the interactive testing of magmatic differentiation models: Computers and Geosciences, v. 4, p. 143-159.

Stout, J. H., 1972, Coexisting amphiboles from Telemark, Norway: Journal of Petrology, v. 13, p. 99-145.

Swanson, S. E., 1977, Relation of nucleation and crystal-growth rate to the development of granitic textures: American Mineralogist, v. 62, p. 966-978.

Teall, J. J. H., 1888, British Petrography: London, Dulau and Co., 469 p.

Truesdell, A. H., 1966, Ion-exchange constants of natural glasses by the electrode method: American Mineralogist, v. 51, p. 110-122.

Tuttle, O. F., and Bowen, N. L., 1958, Origin of granite in the light of experimental studies in the system $NaAlSi_3O_8$-$KAlSi_3O_8$-H_2O: Geological Society of America Mem. 74, 153 p.

Vance, J. A., 1969, On Synneusis: Contributions to Mineralogy and Petrology, v. 24, p. 7-21.

PLATE I

114° 00' 19"
41° 31' 29"

R19W R18W

113° 55' 02"
41° 31' 29

T 9 N

41° 26' 50"
114° 00' 19"

R19W R18W

113° 55' 02"
41° 26' 50"

EXPLANATION

QUATERNARY UNITS

- Qal — Alluvium
- Qco — Colluvium

TERTIARY UNITS

- Tr — Rhyolite
- Trv — Rhyolite vitrophyre
- Td — Dacite
- Tdv — Dacite vitrophyre
- Tpy — Pyroclastic Rocks (bedded ash tuffs, massive tuff breccias)
- Tsl — Salt Lake Formation

SYMBOLS

Contacts, dashed where inferred

D ___ D — Faults, dashed where inferred; D represents downthrown side

45 — Strike and dip of bedding

45 Inclined · Vertical · Horizontal — Strike and dip of flow foliation

UNMAPPED

TN MN 17°

GEOLOGY BY: BRUCE SCARBROUGH, 1984

1/2 0 MILE

1/2 0 KILOMETER

CONTOUR INTERVAL = 20 FEET

A A' 6000' 5500' 5000' Qal Qco Tr Trv Tpy Qco Qal Qco

B B' 6000' 5500' 5000' Qco Qal Tsl ? Td Tr Tdv Td Tr Qco ?

GEOLOGIC MAP OF PARTS OF TOMS CABIN SPRING & LUCIN NW QUADRANGLES (BOX ELDER CO.), UTAH